The effect of single versus successive warm summers on an intertidal community

Amelia V. Hesketh[1,2*], Cassandra A. Konecny[2], Sandra Emry[2], and Christopher D. G. Harley[2,3]

Author affiliations:

1. School of Resource and Environmental Management, Simon Fraser University, 8405 – TASC 1, 8888 University Dr., Burnaby, BC, V5A 1S6
2. Department of Zoology, University of British Columbia, 4200–6270 University Blvd. Vancouver, BC, V6T 1Z4
3. Institute for the Oceans and Fisheries, University of British Columbia, 2202 Main Mall, Vancouver, BC, V6T 1Z4

* Corresponding author: ahesketh@sfu.ca

OPEN RESEARCH STATEMENT:

Data and novel code associated with this manuscript will be made available through Zenodo and Github, respectively, pending acceptance of this manuscript.

KEYWORDS: barnacles; climate change; community; diversity; foundation species; heatwaves; intertidal zone; mortality; repeated stressors; warming

ABSTRACT

To accurately predict how organisms and ecological communities will respond to future conditions caused by climate change, we must consider the temporal dynamics of environmental stressors, including the effects of repeated exposures to stress. We performed a two-year passive warming experiment in coastal British Columbia, Canada to determine how intertidal communities responded to single and successive warm summers. Elevated summer temperatures tended to reduce barnacle and grazer abundance, change algal dynamics, and reduce alpha diversity compared to ambient temperatures, and warming had both contemporaneous and persistent effects. While warm temperatures appeared to have direct effects on organism survival, indirect and persistent effects of warming on community structure and diversity were likely mediated by differences in foundation species (barnacle) abundance between treatments. Unexpectedly, the effects of thermal stress in year two were rarely dependent on whether there had been thermal stress in year one. Our study suggests that, while barnacle beds can recover from single warm summers, recurring thermal stress has cumulative negative effects, resulting in a more depauperate, less diverse community over time, particularly if foundation species are negatively affected.

INTRODUCTION

Just as global mean surface temperatures are expected to increase over the coming decades (IPCC 2023), so, too, are the frequency, severity, and duration of extreme temperature events such as heatwaves (Oliver et al. 2018, Perkins-Kirkpatrick and Lewis 2020). Extreme temperatures have biological consequences. Heatwaves increase the probability of environmental temperatures surpassing the thermal optima and maxima of organisms (Vasseur et al. 2014).

Thus, heatwaves can impair fitness (Siegle et al. 2022) and, ultimately, cause mortality for thermally sensitive species (Harley 2008, Hesketh and Harley 2023), with ramifications for populations, communities, and ecosystems (Harris et al. 2018; Montie and Thomsen 2023).

The effects of heatwaves on organisms are increasingly well-studied; however, the consequences of repeated exposures to thermal stress have received less attention. This is particularly true at the community level, where controlled warming manipulations can present an experimental challenge. If a stressor is prolonged, or if repeated stressors occur in rapid succession, there can be stronger negative consequences on organism survival and fitness (Ma et al. 2018; Siegle et al. 2022), and communities may become more depauperate (Dal Bello et al. 2019) and homogenous (Hammill and Dart 2022). An initial stressor may reduce organismal performance and/or deplete energy stores, engendering susceptibility to subsequent stressors (Marshall and Sinclair 2015, Siegle et al. 2018, Jackson et al. 2021). Alternatively, if an initial stressor increases performance or induces the production of protective metabolites, organisms may instead become more robust to subsequent stressors (Marshall and Sinclair 2015, MacLennan and Vinebrooke 2021, Agrawal and Jurgens 2023). Manipulating the timing of stressors, in addition to their intensity, is needed to understand their ecological effects.

While temperature affects organisms, the reverse is also true. Foundation species, which physically structure ecological communities, often create thermally benign microhabitats for associated organisms (e.g., through moisture retention and shading; Hesketh et al. 2021, Lee et al. 2021, Jurgens et al. 2022, Gutiérrez et al. 2023). The loss of foundation species can thus have profound impacts on communities (Hesketh and Harley 2023; Montie and Thomsen 2023). The importance of such facultative facilitations for bolstering organism survival and performance may increase with environmental stress, though there may be an upper limit beyond which stress

cannot be effectively buffered (Bruno et al. 2003, Bulleri et al. 2016).

Within the intertidal zone, where many species live at or near their thermal maximum (Harley 2011), barnacles are commonly occurring organisms that facilitate a relatively diverse community (Harley 2006, Hesketh et al. 2021). Barnacles can retain moisture (Vermeij 1978, Harley and O'Riley 2011), and provide shade (Cartwright and Williams 2014), thereby reducing the substratum temperature for closely associated species. Even empty barnacle tests provide humid, thermally benign microhabitats for a diverse community (Barnes 2000, Chim et al. 2016). While once considered robust, the resilience of rocky intertidal communities is eroding, in part due to repeated thermal disturbances (Menge et al. 2022). Reduced barnacle abundance and increased barnacle mortality have been attributed to increased thermal stress (Little et al. 2021; Hesketh and Harley 2023), which can also impact the organism abundance within and diversity and composition of associated communities (Kordas et al. 2015, Hesketh and Harley 2023).

Here, we tested the effect of single and successive warm summers on high intertidal barnacle bed communities through a two-year passive warming experiment. Substratum temperatures were manipulated by deploying black (warm) and white (cool) settlement tiles in the intertidal zone (Kordas et al. 2015). After one year, the treatments of half of the experimental tiles were swapped to manipulate the temporal dimension of thermal stress. We hypothesized that, because warming may reduce organism performance and increase mortality, communities exposed to warm temperatures would have lower invertebrate abundance, algal cover, and alpha diversity than those that experienced cool conditions. Further, we expected that warming, because it would reduce foundation species cover, would have persistent indirect negative effects across years. Further, we hypothesized that the effects of warming in the second year of study would be stronger in communities that were previously exposed to warming due to pre-existing

reductions in foundation species cover, and thus reduced availability of thermal refugia.

MATERIALS AND METHODS

Site description

This study was completed near T̓ESNO ̓EN̲ (Beaver Point), a site that lies within the traditional, unceded territory of the W̱SÁNEĆ peoples in what is now known as Ruckle Provincial Park on Salt Spring Island, British Columbia, Canada (48.77324, -123.36637). The substratum at this site is dominated by a southeast-facing semi-exposed sandstone bench, and tides are mixed semi-diurnal. Relative to the rest of British Columbia's Southern Gulf Islands, this area is exposed to cooler, more saline water and larger waves due to its proximity to Haro Strait and the Strait of Juan de Fuca. However, like these and the neighboring San Juan Islands (USA), the intertidal zone at this site is considered a thermal "hot spot" due to its summertime midday low tides coupled with relatively clear, sunny weather (Helmuth et al. 2006).

Here, the upper intertidal zone is dominated by the acorn barnacles *Balanus glandula* and *Chthamalus dalli*, with sporadic beds of the perennial brown alga *Fucus distichus*. Filamentous ephemeral algae (predominantly the green algae *Ulothrix* sp. and *Urospora* sp.) occur as early colonizers of bare space and foliose ephemeral algae occur in winter, often attached to underlying barnacles (predominantly *Ulva* spp., *Pyropia* sp., and *Petalonia fascia*). Dominant herbivores include the littorine snails *Littorina scutulata* and *Littorina sitkana* and the limpets *Lottia paradigitalis* and *Lottia digitalis*, which tend to migrate down shore with the onset of daytime low tides in spring and return to higher tidal elevations in August (Kordas et al. 2015).

Study design

Individual settlement tiles were built based on previous methods (Kordas et al., 2015; see Appendix S1). In brief, each 15x15 cm tile consisted of a central epoxy settlement surface (6.9×6.9 cm, < 5 mm high Sea Goin' Poxy Putty; Permalite Plastics, Rancho Dominguez, CA, USA) bordered by either white (cool treatment) or black (warm treatment) high-density polyethylene (6.4 mm thick; Redwood Plastics, Vancouver, Canada). Temperature differences were driven by differences in the absorption of incoming solar radiation during daytime summer low tides. These settlement tiles were affixed to a bottom tile unit composed of thicker white high-density polyethylene (9.5 mm thick; Redwood Plastics, Vancouver, Canada) that was used to anchor the assembly to the underlying bedrock.

This study followed a randomized block design, with six experimental blocks consisting of eight black and eight white tiles (n = 48). Tiles were installed on 12 April 2019 at a shore level of 2.34 ± 0.07 m above Canadian chart datum. On 3 April 2020, we randomly selected and switched the colour of half of each treatment within each block using white and black heavy-duty tape (Gorilla Tape, Gorilla Glue, Inc., Cincinnati, OH; adhesion enhanced with LePage Ultra Gel super glue). This change resulted in four thermal history treatments during the second year (cool summer–cool summer, CC; cool–warm, CW; warm–cool, WC; and warm–warm, WW; n = 24). Sample size varied over time due to tile damage and dislodgement (Appendix S1: Fig. S3). We initially attempted to also manipulate herbivore communities, but this was abandoned due to wave and temperature regimes at the site (see Appendix S1).

Temperature measurements

For small ectotherms with strong attachment to the substratum (e.g., barnacles), substratum temperature is a reasonably good proxy for body temperature (Kordas et al. 2015). Thus, the substratum temperature of both settlement tiles and adjacent bedrock were collected using pre-programmed iButton temperature loggers (model DS1921G-F5# Thermochron, Dallas Semiconductor). iButtons used to record tile temperatures were sealed in nitrile pouches and sandwiched between the two plates of experimental tile units, while those measuring bedrock temperature were wrapped in Parafilm and affixed to shore with a 2–3 mm layer of A–788 Splash Zone epoxy (Pettit Paints, Rockaway, NJ, USA) separating the logger from both the underlying shore and surrounding air. The number of loggers recording data varied through time for each treatment due to changes in the number of treatment groups between years and instrument failure. In the first and second years, between 3–8 and 1–4 temperature loggers, respectively, were present in each treatment within each block. At least four temperature loggers were always simultaneously recording bedrock temperature across blocks (excepting 18 July–19 August 2020, for which no data exist). Temperatures were recorded hourly except over the second winter of the study, when temperatures were instead recorded every two hours.

Community surveys

Biological communities were characterized through visual surveys, conducted approximately monthly during summer and every two months during winter from 12 April 2019 to 24 February 2021, and by destructive sampling to record epifaunal diversity. During visual surveys, each organism was identified to species except for amphipods and isopods, which were identified to order. Invertebrates were counted, while the percent cover of each alga was

recorded with the aid of a small wire quadrat. Sessile species were only recorded within the central 6×6 cm area of the epoxy settlement surface to avoid edge effects. Motile invertebrates were counted on the entire tile surface since their influence on the experimental community could not be ruled out. We destructively sampled half of the tiles within each treatment and block on 14 September 2020 and sampled remaining tiles on 24 February 2021. All biota were scraped from the settlement surface into containers and preserved in 70% ethanol (v/v in water). Epifauna were identified and counted under a dissecting microscope. Intertidal organisms were collected under Fisheries and Oceans Canada scientific collection permits (XR 61 2019 and XR 196 2020).

Statistical analyses

All analyses were performed in R version 4.3.2 (R core team 2023). We used linear mixed effects models, constructed with *lme4* (Bates et al. 2015), to test for differences in mean daily maximum (MDM) temperature between treatments. Because differences were driven by solar irradiance, temperature data were retained only if they were collected (1) when the tile was emersed (for details, see Appendix S1), (2) after sunrise and before sunset, and (3) during meteorological summer (1 June – 31 August), when treatment differences were likely strongest. Because of frequent logger failures, temperature records for tiles were often incomplete, potentially biasing data. Thus, we calculated both the MDM temperatures of individual loggers and grand MDM temperatures across all loggers. For each date, we subtracted the grand MDM from individual MDM temperatures, generating residual MDM temperatures for each tile. These residuals were modeled as a function of treatment. A random effect of tile number nested within the experimental block was included to account for spatial effects.

We created generalized linear models with *glmmTMB* (Brooks et al. 2017) to test how temperature treatment affected barnacle recruitment and abundance, grazer abundance, and alpha diversity. During the first year, responses were modeled as a function of the treatment (cool or warm), while during the second year, they were modeled as a function of the interaction of treatments applied in year one and year two. Date, when relevant, was included as either an interactive or additive fixed effect, whichever generated the most parsimonious model ($\Delta AIC < 4$). Experimental block was included as a random effect. A fixed effect for initial herbivore manipulations was discarded since this did not substantially improve the fit of any model ($\Delta AIC < 4$). Model fit was evaluated using the *DHARMa* package (Hartig 2022) and ANOVAs were run through the *car* package (Fox and Weisberg 2019) with a significance threshold of $p = 0.05$. Tukey-Kramer *post hoc* pairwise comparisons were performed using *emmeans* (Lenth 2022).

We used generalized additive modeling with the *mgcv* package (Wood 2011) to analyze how the temperature treatments shaped algal cover during each year of the study. Within these models, we included a parametric effect of thermal treatment, a random effect of block, and — to examine temporal trends between treatments — smoothed functions of time for each treatment. Pairwise differences in algal cover over time between control treatments (C or CC) and other treatments were calculated and visualized using established methods (Rose et al. 2012).

Treatment-driven differences in epifaunal community structure and beta diversity were modeled with the *vegan* package (Oksanen et al. 2020). Data were ordinated using distance-based redundancy analysis with Bray-Curtis distances. PERMANOVA analyses were performed with 9999 permutations constrained within experimental blocks. Multiple pairwise comparisons were made with *multiconstrained* in the *BiodiversityR* package (Kindt and Coe 2005). PERMDISP analyses were run with bias adjustment for small sample sizes.

RESULTS

Differences in substratum temperature

Warm treatments had significantly higher residual MDM temperatures than cool treatments during the first summer (Figure 1; ANOVA: $F_{2,72} = 44.88$, $P < 0.001$) and the second summer (ANOVA: $F_{4,69} = 21.00$, $P < 0.001$). In both years, the MDM temperature of warm tiles was ~30.5 ºC, which was 2.4 ºC higher than that of cool tiles (Appendix S1: Table S2). During the second summer, treatments where tape was present on tile surfaces (WC and CW) had similar temperatures to analogous treatments where tape was absent (CC and WW, respectively; Appendix S2: Table S7). Bedrock MDM temperatures were similar to those of warm tiles, but not cool tiles, during the first year (Appendix S2: Table S5) but were similar to those of all treatments during the second year (Appendix S2: Table S7). The MDM, mean, and absolute maximum temperatures within warm and cool treatments were comparable across years (Appendix S1: Table S2).

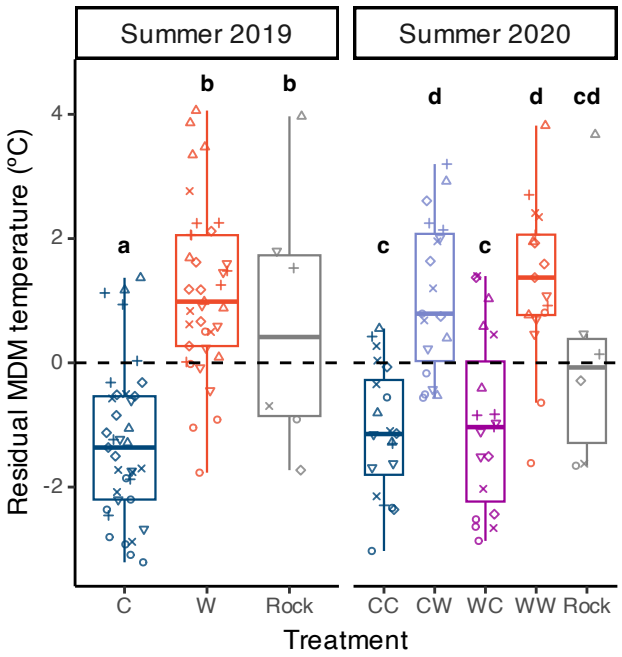

Figure 1. Differences in residual mean daily maximum (MDM) substratum temperatures of experimental tiles and adjacent bedrock recorded by temperature loggers at TESNO, EN. Points represent the mean value for each experimental tile for which temperature was measured, with different shapes used to represent each experiment block. Only temperature data collected during daytime summer low tides between 1 June – 31 August were used. Due to sporadic logger failures, the temperatures of tiles were not necessarily recorded for the entire period, and the number of temperature loggers within each treatment varied over time. Bold lowercase letters represent statistically different groups, as determined by Tukey-Kramer *post hoc* tests on temperature models. C = cool summer, W = warm summer, CC = cool–cool, CW = cool–warm, WC = warm–cool, WW = warm–warm.

Changes in barnacle abundance

Warm summer temperatures tended to cumulatively reduce the abundance of barnacle recruits and adults. When peak recruitment was observed during the first year (May and June, respectively, for *B. glandula* and *C. dalli*), temperature treatment did not significantly affect *B. glandula* recruitment (Fig. 2a; Appendix S2: Table S21), but *C. dalli* recruitment was lower within the warm treatment (Fig. 2b; Type II ANOVA, $\chi^2_1 = 4.13$, $P = 0.0422$). However, at the

241 end of the first year, there were substantially fewer adult *B. glandula* in the warm treatment (Fig.
242 2c; Type II ANOVA; χ^2_1=106.20, $P < 0.001$), while *C. dalli* abundance was similar between
243 treatments (Appendix S2: Table S29). When peak recruitment was observed in the second year,
244 warm temperatures reduced *B. glandula* recruitment, whether warming was applied
245 contemporaneously (Type III ANOVA, treatment_{y2}; χ^2_1=38.34, $P < 0.001$) or during the previous
246 summer (treatment_{y1}; χ^2_1=6.07, $P = 0.0138$). The recruitment of *C. dalli* was similarly negatively
247 affected by warming (Fig. 2d; Type III ANOVA; treatment_{y2}: χ^2_1=19.16, $P < 0.001$; treatment_{y1}:
248 χ^2_1=5.56, $P = 0.0184$). At the end of the study, adult barnacle abundance was not significantly
249 related to warming applied in either year. However, *B. glandula* abundance negatively correlated
250 with warming applied in both summers ($P \sim 0.1$; Appendix S2: Table S27), and *post hoc* testing
251 suggested that *B. glandula* was more abundant in the consistently cool treatment compared to the
252 consistently warm treatment (Tukey-Kramer; z ratio = 3.08, $P = 0.0111$).

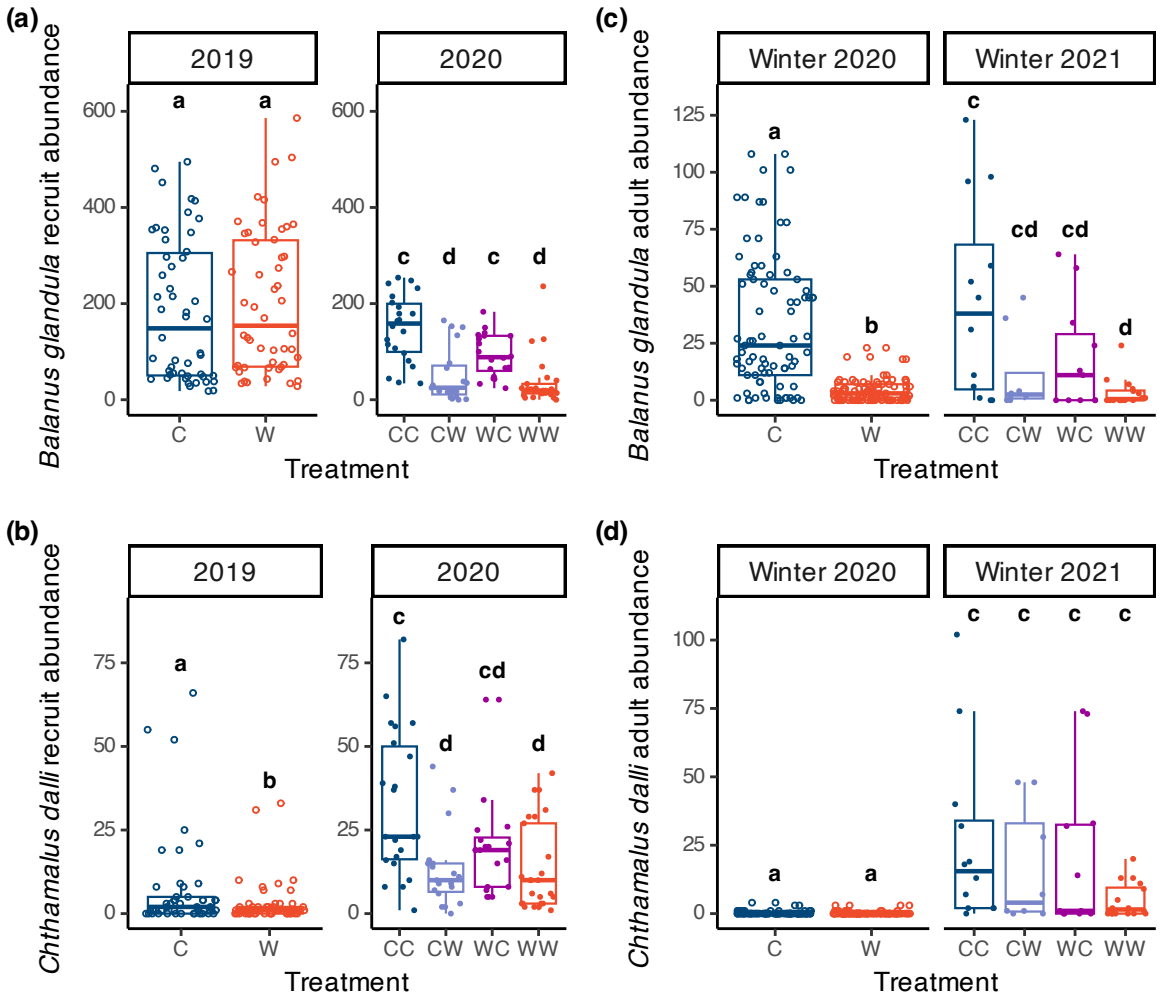

253

254 **Figure 2.** Temperature-driven differences in acorn barnacle abundance on experimental tiles at
255 TESNO, EN, in terms of **(a)** abundance of *B. glandula* and **(b)** *C. dalli* recruits during peak
256 observed recruitment (*B. glandula* 9 May 2019: n = 50; *C. dalli* 5 June 2019: n = 46, 50 for C
257 and W, respectively; 4 June 2020: n = 22, 19, 20, 25 for CC, CW, WC, and WW) and **(c)**
258 abundance of *B. glandula* and **(d)** *C. dalli* adults at the end of the first and second winters
259 (Winter 2020: n=82 for C, n=91 for W; Winter 2021: n = 12, 8, 11, 16 for CC, CW, WC, and
260 WW). Letters indicate significant differences between treatment groups determined by Type II
261 ANOVA (year one) and Tukey-Kramer *post hoc* tests (year two). Treatment codes as in Fig. 1.
262

263

264

265

Changes in grazer abundance

Grazer abundance — which was only modeled during the second year because grazer manipulations were attempted during the first summer — negatively correlated with warming. Both after summer and during winter in the second year, warming applied during the second summer exerted a negative effect on grazer abundance (Fig. 3; Type III ANOVA; $\chi^2_1 = 7.75$, $P < 0.001$ and $\chi^2_1 = 18.97$, $P < 0.001$ for limpets and littorines, respectively). In addition, warming applied during the first summer (WC and WW treatments) had a persistent negative effect on grazer abundance ($\chi^2=4.10$, $P = 0.0428$ and $\chi^2=22.82$, $P <0.001$ for limpets and littorines, respectively). Grazer abundance also changed over time during the second year; limpet abundance significantly increased between the end of summer and the winter ($\chi^2_1=19.21$, $P < 0.001$), but the reverse was true for littorine snails ($\chi^2_1=49.65$, $P < 0.001$).

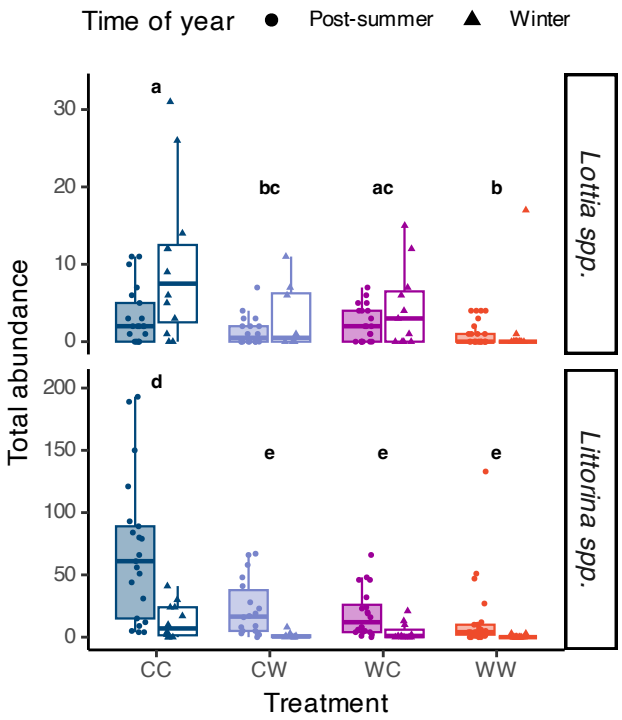

Figure 3. Temperature-driven differences in *Lottia* spp. (limpet) and *Littorina* spp. (littorine snail) abundance on experimental tiles at TESNO¸EN immediately following summer (shaded boxes; September 2020; n = 21, 18, 20, 25 for CC, CW, WC, and WW) and during winter (unshaded boxes; February 2021; n = 12, 8, 11, 16 for CC, CW, WC, and WW). Grazers were counted on the entire 15 x 15 cm upper surface of the tiles. Note different y-axis scales for each taxon. Bold lowercase letters indicate significant differences between treatment groups determined by Tukey-Kramer *post hoc* tests. See Fig. 1 for treatment codes.

Changes in algal cover

The timing of algal blooms and declines differed between treatments, particularly in the first year of study (Figure 4a). Algal cover reached a similar maximum between treatments, driven by a bloom of the green ephemeral alga *Ulothrix* sp. near the end of the first summer. However, the temporal dynamics of algal cover were significantly different between treatments; cover peaked earlier and declined more rapidly within the cool treatment relative to the warm treatment (Fig. 4b; *gamm*; $F_6 = 12.61$, $P < 0.001$). Throughout the second year, algal cover remained similarly low across treatments, though the warm–cool treatment had significantly

greater cover than did the cool–cool treatment by the end of the study ($F_2 = 7.47$, $P = 0.00593$).

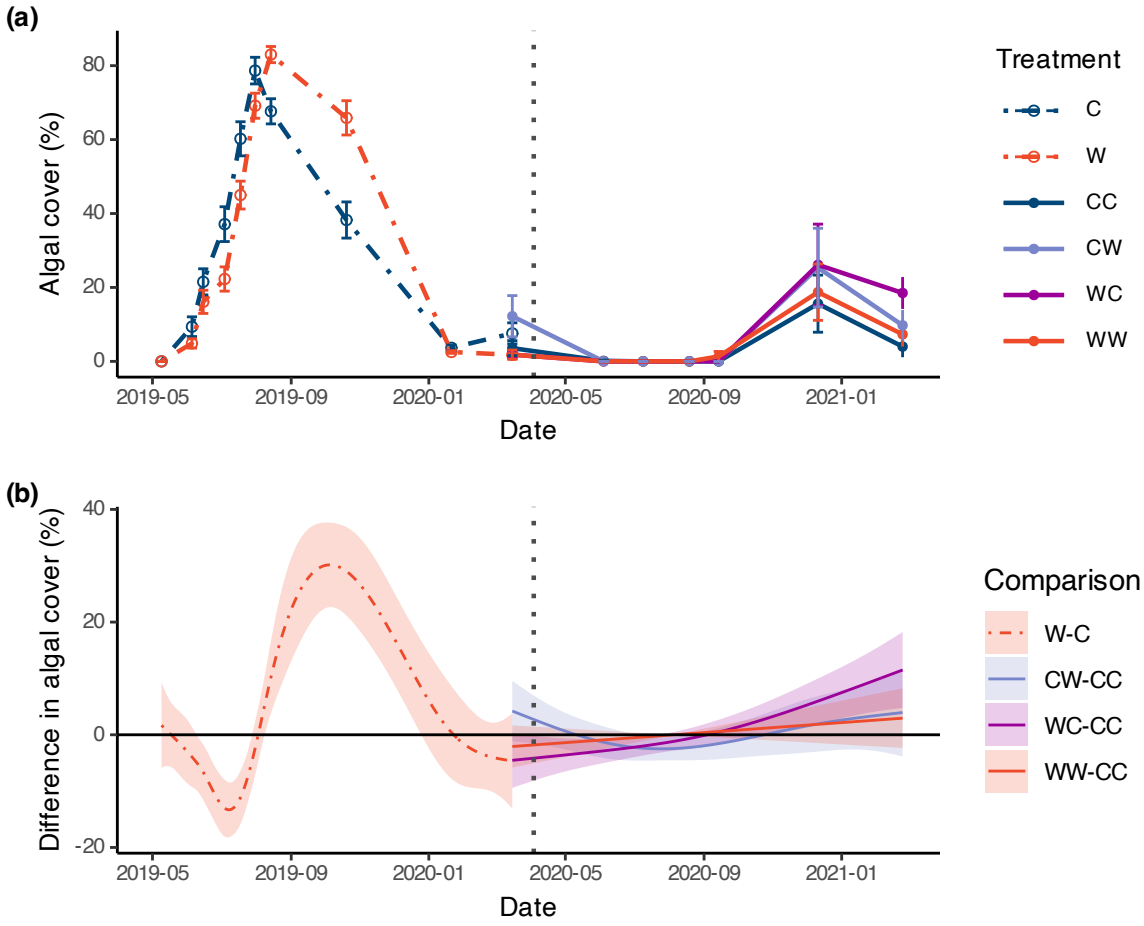

Figure 4. (a) Temperature-driven differences in algal cover on experimental tiles at TESNO, EN. **(b)** Pairwise differences in fitted *gamm* smoothers for algal cover in the control (C or CC) treatment and all other treatments. Shaded areas represent an approximate 95% pointwise confidence interval; when this area does not overlap zero, a significant difference can be inferred. The vertical dotted line represents the date at which treatments were swapped.

Changes in diversity

Warming tended to reduce alpha diversity and alter community structure, particularly in communities that experienced successive warm summers. During the first year, warm

summertime temperatures reduced species richness within communities, and this negative effect was more pronounced in winter than it was immediately after the summer (Fig. 5a; Type III ANOVA; χ^2_1=9.851, P = 0.00170). During the second year, treatment did not significantly affect species richness overall (Fig. 5b; ANOVA; Appendix S2: Table S39). However, *post hoc* pairwise comparisons suggested that treatments which were cool during the second summer different significantly from the treatment that was successively warmed (Tukey-Kramer; CC–WW: z ratio = 4.16, P < 0.0001; WC–WW: z ratio = 3.28, P = 0.00570). Warming exerted a similar negative effect on the Shannon diversity of the invertebrate community; during winter of the first year, diversity was significantly lower within the warm treatment, and during the second year, diversity was lower in treatments where warming was applied during the first year (Appendix S1: Fig. S9a-b, Appendix S2: Tables S41–43). The Shannon diversity of the algal community, meanwhile, was reduced by warm temperatures during the first year, but not during the second year (Appendix S1: Fig. S9c, Appendix S2: Tables S44–46).

Epifaunal communities isolated from destructively sampled tiles demonstrated that community structure, but not beta diversity, differed between treatments. Following the end of the second summer (September 2020; Fig. 5c), differences in community structure were marginally insignificant (PERMANOVA; $F_{3,31}$=1.495, R^2=0.1264, P = 0.0542), though pairwise comparisons indicated the CC and WW treatments differed in composition (*multiconstrained*; F_1=2.705, P = 0.028). By the end of the experiment (February 2021; Fig. 5d), however, communities diverged significantly in their composition among treatments (PERMANOVA; $F_{3,37}$=3.341, R^2=0.2132, P < 0.001). Pairwise comparisons showed that this was primarily driven by differences between the consistently cool treatment and all others, and from differences between the WC and WW treatments (Appendix S2: Table S50). Beta diversity among

communities was similar across treatments (Appendix S2: Tables S51–52). Trends in the alpha diversity of these destructively sampled epifaunal communities were similar to those observed from visual surveys alone (Appendix S1: Figure S10; Appendix S2: Tables S53–56).

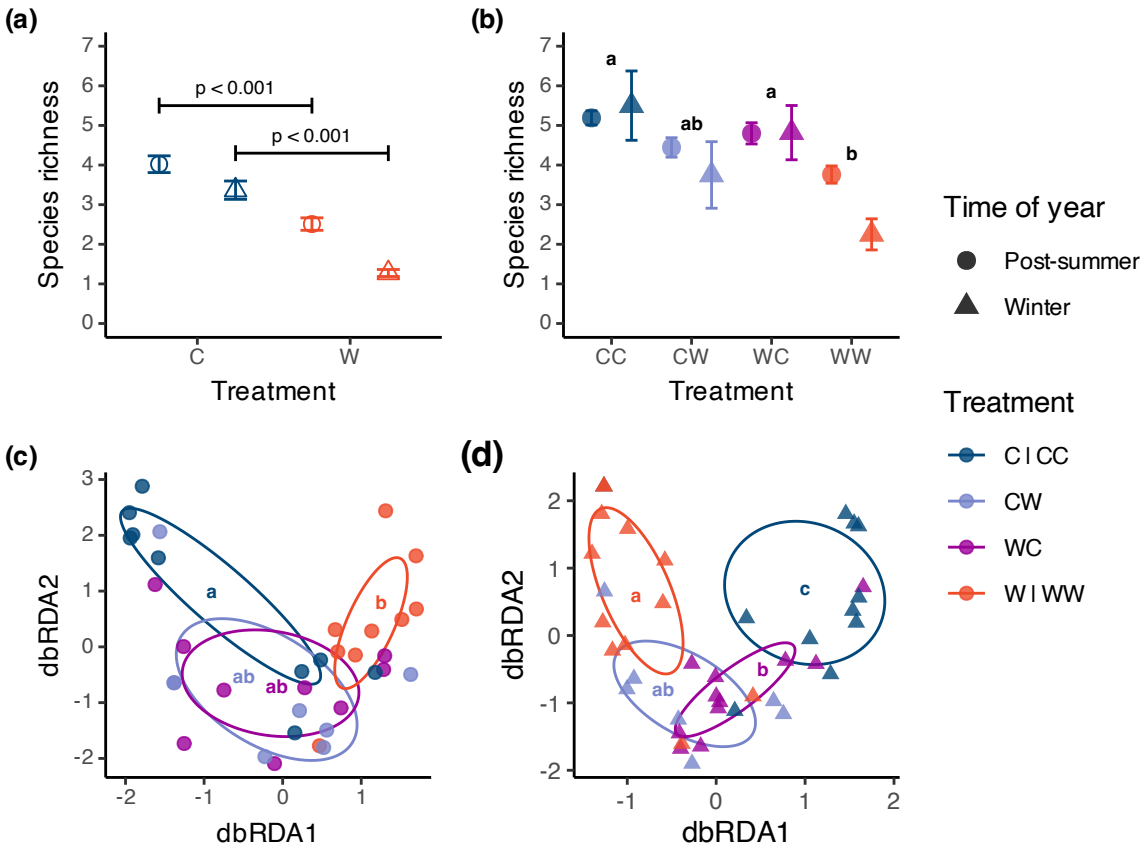

Figure 5. Temperature-driven differences in intertidal community diversity on experimental tiles at TESNO, EN. **(a)** Species richness in year one and **(b)** in year two, determined from visual surveys post-summer and during late winter. Error bars represent standard error about the mean. Symbols/letters denote differences between treatment groups determined by Type II ANOVA (year one) and Tukey-Kramer *post hoc* tests (year two). **(c)** Community structure of destructively sampled epifauna in September 2020 and **(d)** February 2021, plotted in multidimensional space using distance-based redundancy analysis with Bray-Curtis distances. Each point represents a single experimental tile. In year one, n = 47 and 49 for C and W, respectively post-summer and n = 41 and 46 for C and W, respectively, in winter. For year two, n = 21, 18, 20, 25 for CC, CW, WC, and WW post-summer and n = 12, 8, 11, 16 for CC, CW, WC, and WW during winter.

DISCUSSION

In this study, we passively manipulated the substratum temperature of intertidal settlement tiles over two consecutive summers to determine 1) the effect of present and past warming on organism abundance and community diversity and 2) whether prior thermal stress influences the impact of subsequent thermal stress. We expected that warming would have contemporaneous negative effects on organism performance and survival, reducing abundance and diversity, and persistent indirect negative effects mediated by lower foundation species cover. We expected that warming during the second year would have greater negative effects where conditions were previously warm, since foundation species cover and the thermal refugia they create would be constrained, thereby increasing thermal stress for associated biota. As anticipated, we found that warming often had both contemporaneous and persistent negative effects on organism abundance and community alpha diversity, though its effects on algae were more complex. Contrary to our prediction, the effects of warming in the second summer were independent of whether warming had been applied in the first summer.

The methodology employed in this study was effective in manipulating substratum temperatures. In both years, the surfaces of white tiles were cooler than those of black tiles, as in previous studies (Kordas et al. 2015, 2017). Interestingly, bedrock temperatures were more analogous to those of black tiles during the first year. This unexpected pattern could be an artefact of shading from copper fences, which encircled tiles for most of the first summer, but not the second. Despite this, the temperatures of white (cool) and black (warm) tiles were similar between years, as were temperature differences between treatments. These temperature differences were consistently significant, which drove corresponding biological differences.

The abundance of acorn barnacles (*B. glandula* and *C. dalli*) was typically lower within

370 warm treatments, consistent with past studies (Kordas et al. 2015, 2017, Kordas and Harley
371 2016). The dominant barnacle here, *B. glandula*, has an LT_{50} in air between 40.5 ºC (Gilman et
372 al. 2015) and 43 ºC (Hamilton and Gosselin 2020), though mortality has been observed at 40 ºC
373 (Ober et al. 2019). Tile substratum temperatures within all treatments exceeded these lethal
374 thresholds during daytime summer low tides, and warm treatments reached 45 ºC during both
375 years. While barnacles tend to remain slightly cooler than surrounding bedrock (Harley and
376 Lopez 2003), barnacle body temperatures may have surpassed their thermal maximum, causing
377 mortality, particularly within warm treatments. Even exposure to temperatures below critical
378 thermal limits can incur metabolic costs; non-lethal high temperatures can impair *B. glandula*
379 respiration for many hours after exposure (Ober et al. 2019), and sustained warm temperatures
380 can slow barnacle growth (Kordas and Harley 2016). Though elevated temperatures can directly
381 affect barnacle abundance and recruitment, the tendency of barnacles to settle gregariously may
382 magnify these negative effects if warming is sustained. Barnacles preferentially recruit to areas
383 containing conspecifics, a strategy that increases the likelihood of successful sexual reproduction
384 via internal fertilization (Wu 1981). Thus, recruitment to previously warmed tiles during the
385 second year may have been lower because these tiles hosted fewer adult barnacles. The other
386 acorn barnacle present, *C. dalli*, was not prevalent during the first year, possibly due to
387 interannual variation in recruitment dynamics common in barnacles (Scrosati and Ellrich 2016).
388 Recruitment in the second year was lower within warm treatments, but adult survival was
389 unaffected by temperature treatment, possibly because adult *C. dalli* are more robust to thermal
390 stress, with an LT_{50} near 44.5 ºC (Hamilton and Gosselin 2020).
391 Reduced grazer abundance in the warm treatments may have been due to the direct
392 effects of temperature and/or indirect effects mediated by differences in barnacle abundance.

One common limpet in this system, *Lottia digitalis*, has an upper thermal limit of 38 ºC in air (Bjelde and Todgham 2013). High intertidal littorine snails have a slightly greater tolerance to elevated temperatures (41.01 ºC for *L. sitkana* and 41.47 ºC for *L. scutulata* during five-hour emersions; Stickle et al. 2017). While these dominant grazers are thermally robust, recorded summer temperatures frequently exceeded these thresholds for short periods, and temperatures likely regularly fluctuated above grazer thermal optima (e.g., 30 ºC for *L. digitalis*; Bjelde and Todgham 2013), which could have suppressed grazer activity, and thus foraging effectiveness (Rickards and Boulding 2015). Motile organisms can behaviourally thermoregulate by moving to avoid thermal stress. Grazers were not commonly observed on tiles during the summer, though surveys occurred exclusively at low tide, when some grazers avoid feeding (Little 1989), and we may have thus underestimated abundance. However, these temporal dynamics suggest that, while warm temperatures may have directly reduced grazer abundance, indirect effects are more likely. Limpets and littorine snails were generally more abundant within cool treatments where barnacle cover was higher, as has been observed in other studies (Silva et al. 2015, Hesketh et al. 2021). Thus, barnacles may have reduced abiotic stress for these species, as has been shown in previous work (Barnes 2000; Harley and O'Riley 2011; Cartwright and Williams 2014).

Barnacles, in addition to providing microhabitats, may have influenced grazer abundance through their effects on algal food supply. The green filamentous *Ulothrix* sp. dominated bare tiles early in this study. As *Ulothrix* sp. declined towards the end of the first summer, other algal species attached to barnacle tests, predominantly foliose ephemeral algae, became more prevalent, as has been previously observed (Kordas et al. 2017). While maximum algal cover was similar in both temperature treatments during the first year, its temporal dynamics differed; algal cover peaked later and declined more slowly within the warm treatment. High temperatures

416 can have highly variable interspecific effects on algae (Kordas et al., 2017). *Ulothrix* sp. may
417 have persisted through the summer under warm conditions due to higher growth rates or because
418 barnacles, which can compete with algae for space or harbour populations of voracious grazers
419 (Hesketh et al. 2021), were less abundant. On adjacent bedrock, *Ulothrix* sp. was most
420 commonly observed in bare, log-damaged patches within barnacle beds, supporting an indirect
421 negative effect of barnacles on this species (as has been documented with the ephemeral green
422 alga *Urospora* spp.; Harley 2006). Meanwhile, other algae may preferentially attach to rugose
423 barnacle tests (here, *Pyropia* sp. and *Ulva* sp.), and barnacles can provide refuge from
424 desiccation and grazing for algal spores and germlings (Farrell 1991; Geller 1991). Thus, algal
425 cover may have been highest in the warm-cool treatment during the second year because shifting
426 thermal conditions created a heterogenous mixture of bare space and sparse barnacles, allowing
427 for the growth of both heat-tolerant, barnacle-phobic and heat-intolerant, barnacle-philic algae.
428 Alpha diversity generally increased over the course of succession, tending to decline in
429 spring and remain low in summer, particularly within warm treatments, as has been previously
430 found (Kordas et al. 2015, Kordas et al. 2017). Barnacle recruits, followed by opportunistic
431 ephemeral algae, appeared shortly after tiles were installed, consistent with studies involving
432 intertidal disturbance and succession in the northeast Pacific (Farrell 1991, Geller 1991).
433 Because barnacles act as both facilitators (Farrell 1991) and food sources (Harley and O'Riley
434 2011), their presence allowed grazers (e.g., amphipods, polychaete worms), secondary
435 successional species (e.g., perennial algae), and predators (e.g., ribbon worms) to enter the
436 nascent community. Thus, the higher alpha diversity of cool compared to warm treatments may
437 have been driven by barnacle facilitation, by more species surviving under thermally benign
438 conditions, or — more likely — by a mixture of these two mechanisms. Disentangling these

indirect and direct effects is challenging given the experimental design employed.

Because foundation species (barnacle) cover was lower within the warm treatment compared to the cool treatment after the first year, we anticipated that the effects of warming would be magnified during the second year. However, the negative effect of warming in the second summer was independent of warming in the first year. While intertidal foundation species can improve the survival, growth, and diversity of associated species in the face of thermal stress (Cartwright and Williams 2014; Jurgens et al. 2022; Hesketh and Harley 2023), the size and density of foundation species can affect their facilitative ability (Yang et al. 2017; Irving and Bertness 2009). These acorn barnacles, while they facilitated biodiversity, may have been too small or sparse to effectively buffer thermal stress (Rickards and Boulding 2015).

While intertidal systems are resilient up to a point, repeated atmospheric warming threatens to disrupt even these historically stalwart communities (Menge et al. 2022). Our results suggest that even for high-turnover barnacle bed communities (Farrell 1991), warming generates lasting effects on community structure through reduced barnacle density. As mean temperatures increase with climate change, so, too, may heatwaves (Oliver et al. 2018; Perkins-Kirkpatrick and Lewis 2020), which may cause mortality (Hesketh and Harley 2023) and accelerate shifts in ecological communities (Harris et al. 2018). Climate change also encompasses multiple stressors beyond temperature, and these may co-occur and interact with warming (MacLennan and Vinebrooke 2021). To understand the full risk of climate change to ecological communities, we must embrace complexity by integrating stochasticity, considering the temporal dimensions of stress, and otherwise seeking to emulate natural processes within our experimental designs.

CONFLICT OF INTEREST: The authors declare no conflicts of interest.

ACKNOWLEDGEMENTS: We acknowledge and thank the Coast Salish peoples on whose traditional, sovereign, and unceded territory this work was conducted. We thank S. Blain, A. Holland, and G. Brownlee for assistance with field work, B. Gillespie and V. Grant for assistance with tile construction, and BC Parks for foreshore access. Thanks to R. Kordas for her prior work, and R. Germain, C. Brauner, and S. Dudas for feedback on early drafts. National Geographic provided funding through AVH (EC-54154R-18). Additional support was provided to CDGH through Canadian Healthy Oceans Network (NETGP 468437-14) and an NSERC Discovery Grant (RGPIN-2016-05441).

REFERENCES

Agrawal, A. and Jurgens, L. J. 2023. Effects of asynchronous stressors on the eastern oyster (*Crassostrea virginica*). Estuaries and Coasts 46: 697–706.

Barnes, M. 2000. The use of intertidal barnacle shells. In: Oceanography and Marine Biology: an Annual Review. Taylor & Francis, pp. 157–187.

Bates, D., Mächler, M., Bolker, B. and Walker, S. 2015. Fitting linear mixed-effects models using lme4. Journal of Statistical Software 67: 1–48.

Bjelde, B. E. and Todgham, A. E. 2013. Thermal physiology of the fingered limpet *Lottia digitalis* under emersion and immersion. Journal of Experimental Biology 216: 2858–2869.

Brooks, M.E., Kristensen, K., van Benthem, K.J., Magnusson, A., Berg, C.W., Nielsen, A., Skaug, H.J., Maechler, M. and Bolker, B.M. 2017. glmmTMB balances speed and flexibility among packages for zero-inflated generalized linear mixed modeling. The R Journal 9: 378400

Bruno, J. F., Stachowicz, J. J. and Bertness, M. D. 2003. Inclusion of facilitation into ecological theory. Trends in Ecology & Evolution 18: 119–125.

485 Bulleri, F., Bruno, J. F., Silliman, B. R. and Stachowicz, J. J. 2016. Facilitation and the niche:
486 implications for coexistence, range shifts and ecosystem functioning. Functional Ecology 30:
487 70–78.
488 Cartwright, S. R. and Williams, G. A. 2014. How hot for how long? The potential role of heat
489 intensity and duration in moderating the beneficial effects of an ecosystem engineer on rocky
490 shores. Marine Biology 161: 2097–2105.
491 Chim, C. K., Wong, H. P.-S. and Tan, K. S. 2016. *Tetraclita* (Cirripedia, Thoracica) tests as an
492 important habitat for intertidal isopods and other marine and semi-terrestrial fauna on tropical
493 rocky shores. Crustaceana 89: 985–1040.
494 Dal Bello, M., Rindi, L. and Benedetti-Cecchi, L. 2019. Temporal clustering of extreme climate
495 events drives a regime shift in rocky intertidal biofilms. Ecology 100: e02578.
496 Farrell, T. M. 1991. Models and mechanisms of succession: An example from a rocky intertidal
497 community. Ecological Monographs 61: 95–113.
498 Fox, J. and Weisberg, S. 2019. An {R} companion to applied regression, third edition. Thousand
499 Oaks CA: Sage.
500 Geller, J. B. 1991. Gastropod grazers and algal colonization on a rocky shore in northern
501 California: the importance of the body size of grazers. Journal of Experimental Marine
502 Biology and Ecology 150: 1–17.
503 Gilman, S., Hayford, H., Craig, C. and Carrington, E. 2015. Body temperatures of an intertidal
504 barnacle and two whelk predators in relation to shore height, solar aspect, and microhabitat.
505 Marine Ecology Progress Series 536: 77–88.
506 Gutiérrez, J. L., Bagur, M., Lorenzo, R. A. and Palomo, M. G. 2023. A facultative mutualism
507 between habitat-forming species enhances the resistance of rocky shore communities to heat

waves. – Frontiers in Ecology and Evolution 11: 1278762.

Hamilton, H. and Gosselin, L. 2020. Ontogenetic shifts and interspecies variation in tolerance to desiccation and heat at the early benthic phase of six intertidal invertebrates. Marine Ecology Progress Series 634: 15–28.

Hammill, E. and Dart, R. 2022. Contributions of mean temperature and temperature variation to population stability and community diversity. Ecology and Evolution 12: e8665.

Harley, C. D. G. and Lopez, J. P. 2003. The natural history, physiology, and ecological impacts of the intertidal mesopredators, *Oedoparena* spp. (Diptera, Dryomyzidae). Invertebrate Biology 122:61-73

Harley, C. D. G. 2006. Effects of physical ecosystem engineering and herbivory on intertidal community structure. Marine Ecology Progress Series 317: 29–39.

Harley, C. 2008. Tidal dynamics, topographic orientation, and temperature-mediated mass mortalities on rocky shores. Marine Ecology Progress Series 371: 37–46.

Harley, C. D. G. 2011. Climate change, keystone predation, and biodiversity loss. Science 334: 1124–1127.

Harley, C. D. G. and O'Riley, J. L. 2011. Non-linear density-dependent effects of an intertidal ecosystem engineer. Oecologia 166: 531–541.

Harris, R. M. B., Beaumont, L. J., Vance, T. R., Tozer, C. R., Remenyi, T. A., Perkins-Kirkpatrick, S. E., Mitchell, P. J., Nicotra, A. B., McGregor, S., Andrew, N. R., Letnic, M., Kearney, M. R., Wernberg, T., Hutley, L. B., Chambers, L. E., M-S, F., Keatley, M. R., Woodward, C. A., Williamson, G., Duke, N. C., and Bowman, D. M. J. S. 2018. Biological responses to the press and pulse of climate trends and extreme events. Nature Climate Change 8: 579–587.

Hartig, F. 2021. DHARMa: Residual diagnostics for hierarchical (multi-level/mixed) regression models. R package version 0.4.6.

Helmuth, B., Broitman, B. R., Blanchette, C. A., Gilman, S., Halpin, P., Harley, C. D. G., O'Donnell, M. J., Hofmann, G. E., Menge, B. and Strickland, D. 2006. Mosaic patterns of thermal stress in the rocky intertidal zone: Implications for climate change. Ecological Monographs 76: 461–479.

Hesketh, A. V. and Harley, C. D. G. 2023. Extreme heatwave drives topography-dependent patterns of mortality in a bed-forming intertidal barnacle, with implications for associated community structure. Global Change Biology 29: 165–178.

Hesketh, A. V., Schwindt, E. and Harley, C. D. G. 2021. Ecological and environmental context shape the differential effects of a facilitator in its native and invaded ranges. Ecology 102: e03478.

IPCC. 2023. Climate Change 2023: Synthesis Report. Contribution of Working Groups I, II and III to the Sixth Assessment Report of the Intergovernmental Panel on Climate Change (Core Writing Team, Lee, H. and Romero, J., Eds.) IPCC, Geneva, Switzerland, pp. 35–115.

Irving, A. D., Bertness, M. D. 2009. Trait-dependent modification of facilitation on cobble beaches. Ecology 90: 3042–3050.

Jackson, M. C., Pawar, S. and Woodward, G. 2021. The temporal dynamics of multiple stressor effects: From individuals to ecosystems. Trends in Ecology & Evolution 36: 402–410.

Jurgens, L. J., Ashlock, L. W. and Gaylord, B. 2022. Facilitation alters climate change risk on rocky shores. Ecology 103: e03596.

Kindt, R. and Coe, R. 2005. Tree diversity analysis. A manual and software for common statistical methods for ecological and biodiversity studies. Nairobi: World Agroforestry Centre

(ICRAF).

Kordas, R. and Harley, C. 2016. Demographic responses of coexisting species to *in situ* warming. Marine Ecology Progress Series 546: 147–161.

Kordas, R. L., Dudgeon, S., Storey, S. and Harley, C. D. G. 2015. Intertidal community responses to field-based experimental warming. Oikos 124: 888–898.

Kordas, R. L., Donohue, I. and Harley, C. D. G. 2017. Herbivory enables marine communities to resist warming. Science Advances 3: e1701349.

Lee, R. H., Morgan, B., Liu, C., Fellowes, J. R. and Guénard, B. 2021. Secondary forest succession buffers extreme temperature impacts on subtropical Asian ants. Ecological Monographs 91: e01480.

Lenth, R. 2023. emmeans: Estimated marginal means, aka least-squares means. R package version 1.8.6.

Little, C. 1989. Factors governing patterns of foraging activity in littoral marine herbivorous molluscs. Journal of Molluscan Studies 55: 273–284.

Little, C., Trowbridge, C. D., Williams, G. A., Hui, T. Y., Pilling, G. M., Morritt, D. and Stirling, P. 2021. Response of intertidal barnacles to air temperature: Long-term monitoring and *in-situ* measurements. Estuarine, Coastal and Shelf Science 256: 107367.

Ma, C.-S., Wang, L., Zhang, W. and Rudolf, V. H. W. 2018. Resolving biological impacts of multiple heat waves: interaction of hot and recovery days. Oikos 127: 622–633.

MacLennan, M. M. and Vinebrooke, R. D. 2021. Exposure order effects of consecutive stressors on communities: the role of co-tolerance. Oikos 130: 2111–2121.

Marshall, K. E. and Sinclair, B. J. 2015. The relative importance of number, duration and intensity of cold stress events in determining survival and energetics of an overwintering insect.

577 Functional Ecology 29: 357–366.
578 Menge, B. A., Gravem, S. A., Johnson, A., Robinson, J. W. and Poirson, B. N. 2022. Increasing
579 instability of a rocky intertidal meta-ecosystem. Proceedings of the National Academy of
580 Sciences U.S.A. 119: e2114257119.
581 Montie, S. and Thomsen, M. S. 2023. Long-term community shifts driven by local extinction of
582 an iconic foundation species following an extreme marine heatwave. Ecology and Evolution
583 13: e10235.
584 Ober, G., Rognstad, R. and Gilman, S. 2019. The cost of emersion for the barnacle *Balanus*
585 *glandula*. Marine Ecology Progress Series 627: 95–107.
586 Oliver, E. C. J., Donat, M. G., Burrows, M. T., Moore, P. J., Smale, D. A., Alexander, L. V.,
587 Benthuysen, J. A., Feng, M., Sen Gupta, A., Hobday, A. J., Holbrook, N. J., Perkins-
588 Kirkpatrick, S. E., Scannell, H. A., Straub, S. C. and Wernberg, T. 2018. Longer and more
589 frequent marine heatwaves over the past century. Nature Communications 9: 1324.
590 Oksanen, J., Blanchet, F.G., Friendly, M., Kindt, R., Legendre, P., McGlinn, D., Minchin, P.R.,
591 O'Hara, R. B., Simpson, G.L., Solymos, P., Stevens, M.H.H., Szoecs, E. and Wagner, H. 2020.
592 vegan: Community Ecology Package. R package version 2.6-4.
593 Perkins-Kirkpatrick, S. E. and Lewis, S. C. 2020. Increasing trends in regional heatwaves.
594 Nature Communications 11: 3357.
595 Rickards, K. and Boulding, E. 2015. Effects of temperature and humidity on activity and
596 microhabitat selection by *Littorina subrotundata*. Marine Ecology Progress Series 537: 163–
597 173.
598 Rose, N. L., Yang, H., Turner, S. D. and Simpson, G. L. 2012. An assessment of the mechanisms
599 for the transfer of lead and mercury from atmospherically contaminated organic soils to lake

sediments with particular reference to Scotland, UK. Geochimica et Cosmochimica Acta 82: 113–135.

Scrosati, R. A. and Ellrich, J. A. 2016. A 12-year record of intertidal barnacle recruitment in Atlantic Canada (2005–2016): Relationships with sea surface temperature and phytoplankton abundance. PeerJ 4: e2623–e2623.

Siegle, M. R., Taylor, E. B. and O'Connor, M. I. 2018. Prior heat accumulation reduces survival during subsequent experimental heat waves. Journal of Experimental Marine Biology and Ecology 501: 109–117.

Siegle, M. R., Taylor, E. B. and O'Connor, M. I. 2022. Heat wave intensity drives sublethal reproductive costs in a tidepool copepod. Integrative Organismal Biology 4: obac005.

Silva, A. C. F., Mendonça, V., Paquete, R., Barreiras, N. and Vinagre, C. 2015. Habitat provision of barnacle tests for overcrowded periwinkles. Marine Ecology 36: 530–540.

Stickle, W. B., Carrington, E. and Hayford, H. 2017. Seasonal changes in the thermal regime and gastropod tolerance to temperature and desiccation stress in the rocky intertidal zone. Journal of Experimental Marine Biology and Ecology 488: 83–91.

Vasseur, D. A., DeLong, J. P., Gilbert, B., Greig, H. S., Harley, C. D. G., McCann, K. S., Savage, V., Tunney, T. D. and O'Connor, M. I. 2014. Increased temperature variation poses a greater risk to species than climate warming. Proceedings of the Royal Society B. 281: 20132612.

Vermeij, G. J. 1978. Biogeography and Adaptation: Patterns of Marine Life. Harvard University Press.

Wood, S. N. 2011. Fast stable restricted maximum likelihood and marginal likelihood estimation of semiparametric generalized linear models. Journal of the Royal Statistical Society (B) 73: 3–

623 36.
624 Wu, R. S.-S. 1981. The effect of aggregation on breeding in the barnacle *Balanus glandula*,
625 Darwin. Canadian Journal of Zoology 59: 890–892.
626 Yang, Y., Chen, J.-G., Schöb, C. and Sun, H. 2017. Size-mediated interaction between a cushion
627 species and other non-cushion species at high elevations of the Hengduan Mountains, SW
628 China. Frontiers in Plant Science 8: 465.
629

APPENDIX S1: ADDITIONAL METHODS AND RESULTS

The effect of single versus successive warm summers on an intertidal community

Amelia V. Hesketh, Cassandra A. Konecny, Sandra M. Emry, Christopher D. G. Harley

Tile construction

Experimental tiles consisted of a sandwich of two 15 x 15 cm squares of high-density polyethylene "puckboard" (Redwood Plastics, BC). The bottom tile (white, 9.5 mm thickness) was used to anchor the tile assembly to the underlying bedrock using two 18-8 stainless steel lag bolts (6.35 x 38.1 mm; Pacific Fasteners, BC). The lag bolts were threaded through 9.5 mm holes (with a 1.91 cm counterbore) drilled along the centre line of the bottom tile unit and screwed into plastic anchors (6.35 x 38.1 mm High-Strength Twist-Resistant Plastic Anchors for Block and Brick; McMaster-Carr, IL) set within 7.94 mm diameter holes drilled into the underlying bedrock. Four tee nuts were hammered into each of four 9.5 mm holes in the corners of the bottom tile unit, and button screws were threaded through 6.35 mm interior diameter stainless steel lock washers (Pacific Fasteners, BC) and corresponding 6.35 mm holes in the top tile units to facilitate assembly. A central 2.06 cm hole was drilled through the top tile to allow an iButton temperature logger to be installed within the experimental tile unit. To enhance epoxy adhesion while constructing the settlement area, 12–6.4 mm holes were drilled within the central 6.9 x 6.9 cm area of the top tile unit, and this area was sanded. We placed a circle of cork within the central hole before spreading a thin layer (≤ 5 mm) of Sea Goin' Poxy Putty (Permalite Plastics, Rancho Dominguez, CA) over the area. To enhance fine-scale heterogeneity of the surface, we pressed finely ground Epsom salts into the putty. Once the epoxy dried, the Epsom salts were dissolved with tap water, leaving behind fine pock marks on the settlement surface, and the cork

was removed from the central hole to create a cavity for the temperature logger. See Fig. S1 for a detailed diagram.

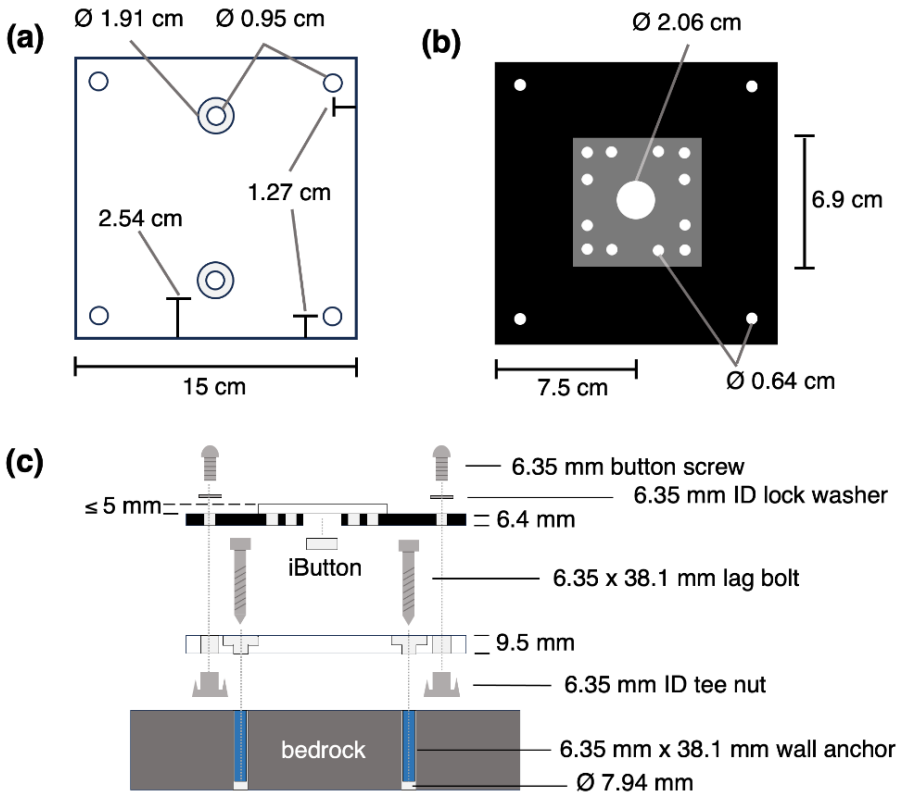

Figure S1. Diagrams of representative tile assembly used for testing the effect of artificial warming on barnacle bed communities. **(a)** Bottom unit of tile assembly, viewed from top without hardware installed. **(b)** Top unit of tile, in this case a black (warm) treatment tile, viewed from the top without hardware installed. The transparent square represents the central epoxy settlement area overlying the tile. **(c)** Exploded view of tile including hardware for assembly and installation, viewed from the side. ø = diameter, ID = interior diameter. The exact position of the holes, absent the central hole for the iButton temperature logger, was not measured, so these positions have been approximated from photographs.

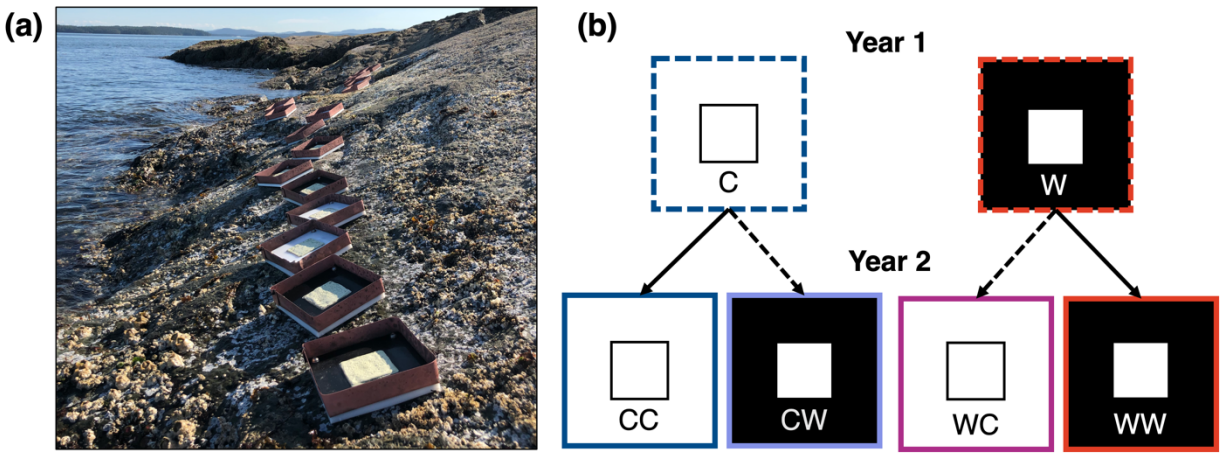

Figure S2. Experimental tiles and experimental design for testing how single versus successive warm summers affected intertidal barnacle bed communities at TESNO¸EN, Salt Spring Island. **(a)** Photograph of experimental tiles anchored in the intertidal zone, still with copper fences attached to facilitate grazer manipulations. **(b)** Schematic of experimental design, wherein black (W=warm) and white (C=cool) settlement tiles were monitored for one year before swapping the treatment for half of each group of tiles (indicated by dashed arrows), generating four treatments for the second year of the study (CC = cool summer – cool summer; CW = cool summer – warm summer; WC = warm summer – cool summer; WW = warm summer – cool summer).

Changes to experimental design

In April 2019, we installed five blocks of 20 tiles each, half of which were white and half of which were black (N=100) at a shore level of 2.27 ± 0.06 m (mean ± SE) above Canadian chart datum. However, due to floating log disturbance within some of the blocks, several tiles were lost. In June 2019, we relocated tiles to more suiTable Sreas to prevent log disturbance from causing further losses, expanding the experiment to six experimental blocks with approximately 16 tiles each, eight black and eight white where blocks were balanced (N=96). All tiles were re-installed at a similar shore level of 2.34 ± 0.07 m.

We originally intended to manipulate herbivore community diversity on the experimental tiles to test how grazer diversity influences resilience to warming, an effort that was ultimately abandoned due to the ineffectiveness of copper fences at controlling the abundance of some

species, thermal stress killing others, and frequent log disturbance crushing copper fences. From March–August 2019, copper fences were affixed around each experimental tile (0.511 mm thick, 3.8 cm high above the level of the tile; Fig. S2). Different combinations of grazers (using *Littorina sitkana*, *Littorina scutulata*, *Lottia digitalis*, and *Lottia paradigitalis*) were established on each tile: all four grazers, all three combinations of three grazers, each grazer alone, and no grazers. Despite the presence of copper fences, littorine snails — perhaps aided by wave action — were nonetheless readily able to move on and off of the tiles. A pivot to limpet-only treatment combinations (using both previously mentioned *Lottia* spp. and *Lottia scutum*) in June 2019 was also unsuccessful, as mortality in most limpet species was very high, likely due to thermal stress on the still relatively bare tiles. What limpets of these species did survive during this period were often found at the edges of tiles or wedged in the cracks between the tile and copper fence, and thus their biological function within tile communities was likely minimal. In August 2019, we thus removed the copper fences, and herbivores of all species were allowed unfettered access to tile communities thereafter.

Table S1. Design iterations employed during study of passive summertime warming on barnacle bed communities at TESNO, EN. Treatments were applied from initial establishment in March 2019 to the experiment endpoint in February 2021.

Iteration	Time period	Manipulations	Treatments	Blocks	n	Reason for change
1	April–June 2019	Temperature · herbivory (2 limpets + 2 littorines)	2 · 10 = 20	5	5	Littorine movement
2	June–August 2019	Temperature · herbivory (3 limpet spp.)	2 · 8 = 16	6	6	Log disturbance, thermal stress
3	August 2019–February 2021	Temperature · time	2 · 2 = 4	6	24	

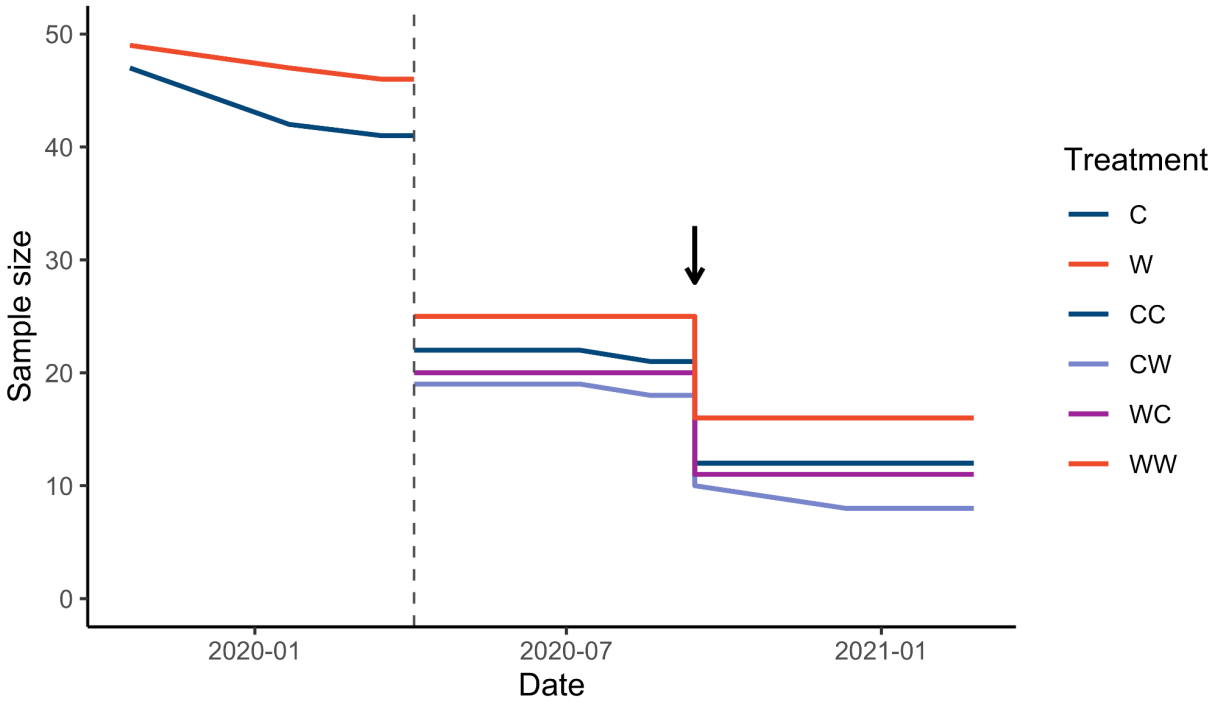

Figure S3. Changes in the number of experimental tiles within treatment groups over time. The time series begins after the end of early herbivore manipulations. The dashed vertical line indicates when year two tile treatments (CC, CW, WC, WW) were established by reversing the color of half of the tiles, at which point sample sizes were effectively halved, and the arrow indicates when the first set of tiles was destructively sampled to measure epifaunal abundance and community structure in September 2020. See Fig. S2 for treatment abbreviations.

Estimating tile shore levels

Shore levels for individual tiles were estimated from temperature traces and tide data (Fisheries and Oceans Canada 2022). For each tile, temperature data from spring low tide series during the middle of summer were manually searched for three intervals where temperatures clearly transitioned from moderate sea surface temperatures one hour (typically ~12–15 ºC) to much higher aerial temperatures (>20 ºC) the next. These transitions occur when tiles become emersed after being immersed. The shore level of the tile above Canadian chart datum was approximated as the mean level of the tide between those two timepoints. These shore level values were subsequently used in filtering temperature data for plotting and analyses.

Additional temperature data

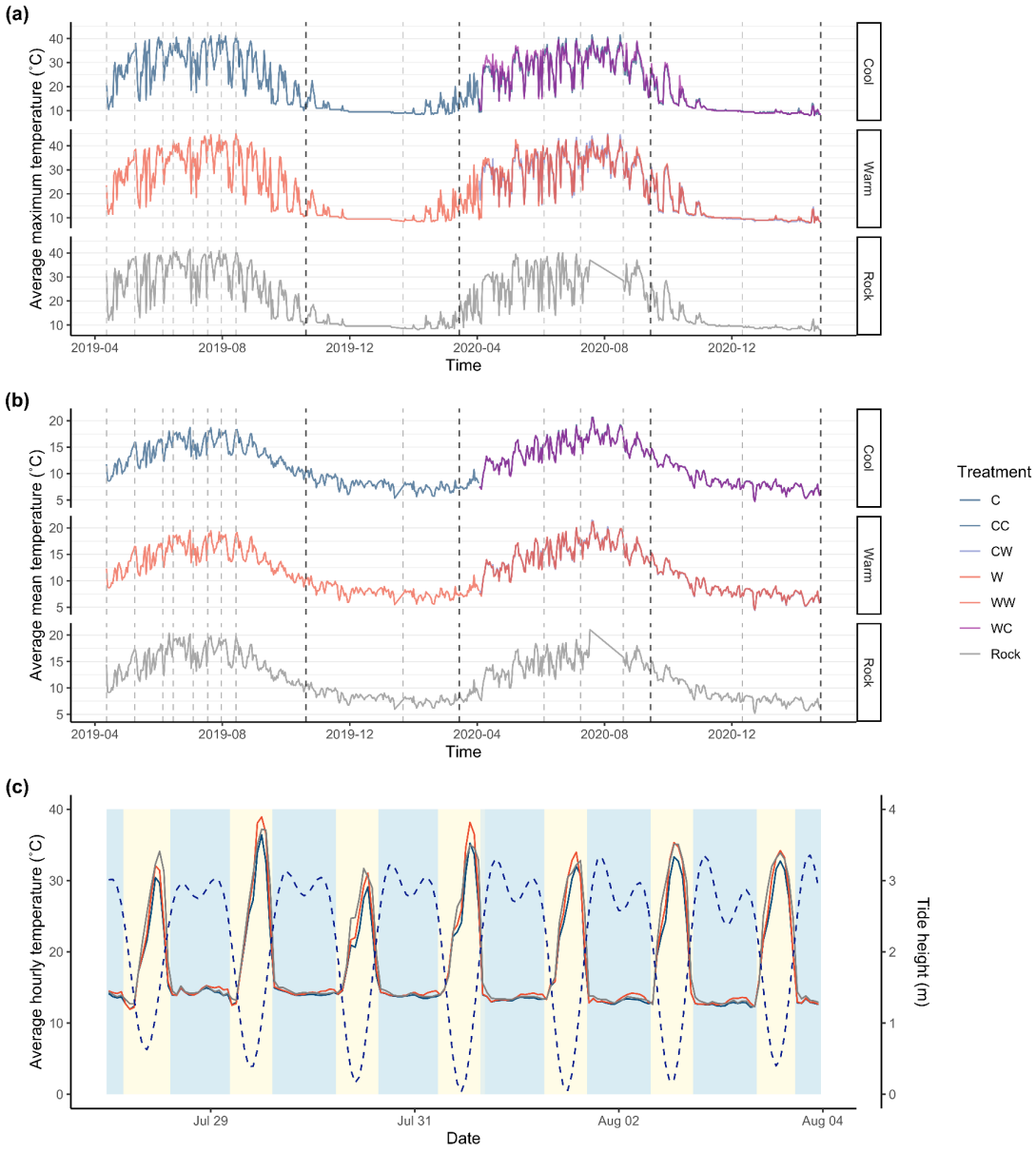

Figure S4. Temperatures of experimental tile and adjacent bedrock, as recorded by iButton temperature loggers during a two-year passive warming experiment at TESNO, EN, Salt Spring Island. **(a)** Mean daily maximum and **(b)** mean temperatures over the entire experiment, averaged for each treatment. Dashed vertical lines represent when visual surveys were performed, with darker lines representing data for which post-summer and post-winter analyses were conducted. **(c)** Hourly temperature data collected between 28 July 2019 and 4 August 2019 averaged among all tiles in each treatment. Tide data are overlaid (height above Canadian chart datum; dashed line) to illustrate the effect of emersion (pale yellow background) and submersion (pale blue background). Treatment abbreviations as in Fig. S2.

Warm treatments had higher MDM temperatures than cool treatments in both year one (Fig. S5a; ANOVA; $F_{2,72} = 45.04$, $P < 0.001$) and year two (ANOVA; $F_{2,69} = 20.96$, $P < 0.001$). Trends were similar for mean temperature (Fig. S5b; ANOVA; year one: $F_{2,73} = 45.53$, $P < 0.001$; year two: $F_{4,68} = 21.17$, $P < 0.001$). MDM and mean bedrock temperatures were more similar to the warm treatment during the first year and more similar to the cool treatments in the second year (Table S10). The maximum temperature reached within the warm treatment was higher than that of the cool treatment and bedrock during both year one (Fig. S5c; $F_{2,73} = 33.46$, $P < 0.001$) and year two ($F_{4,71} = 8.38$, $P < 0.001$; Table S14).

Table S2. Thermal conditions on experimental tiles deployed during a two-year passive warming experiment at TESNO, EN. Temperature data reflect only those data recorded during summertime low tides, and may suffer from thermal bias since temperature records were often incomplete for individual loggers. Abbreviations as in Fig. A2. MDM = mean daily maximum, values are reported ± one standard deviation.

Period	Treatment	MDM temperature (ºC)	Mean temperature (ºC)	Maximum temperature (ºC)
	C	28.2 ± 6.2	22.1 ± 4.3	38.5 ± 1.8
Year 1	W	30.4 ± 6.3	24.2 ± 4.9	41.7 ± 1.8
	Rock	30.6 ± 7.2	23.5 ± 5.0	38.2 ± 2.5
	CC	28.0 ± 5.9	21.8 ± 4.5	37.3 ± 2.9
	WC	28.0 ± 5.8	21.9 ± 4.6	37.7 ± 1.7
Year 2	CW	30.3 ± 6.6	23.2 ± 5.0	40.5 ± 2.7
	WW	30.6 ± 6.6	23.4 ± 5.2	40.3 ± 2.2
	Rock	27.5 ± 6.2	21.8 ± 4.8	38.0 ± 1.8

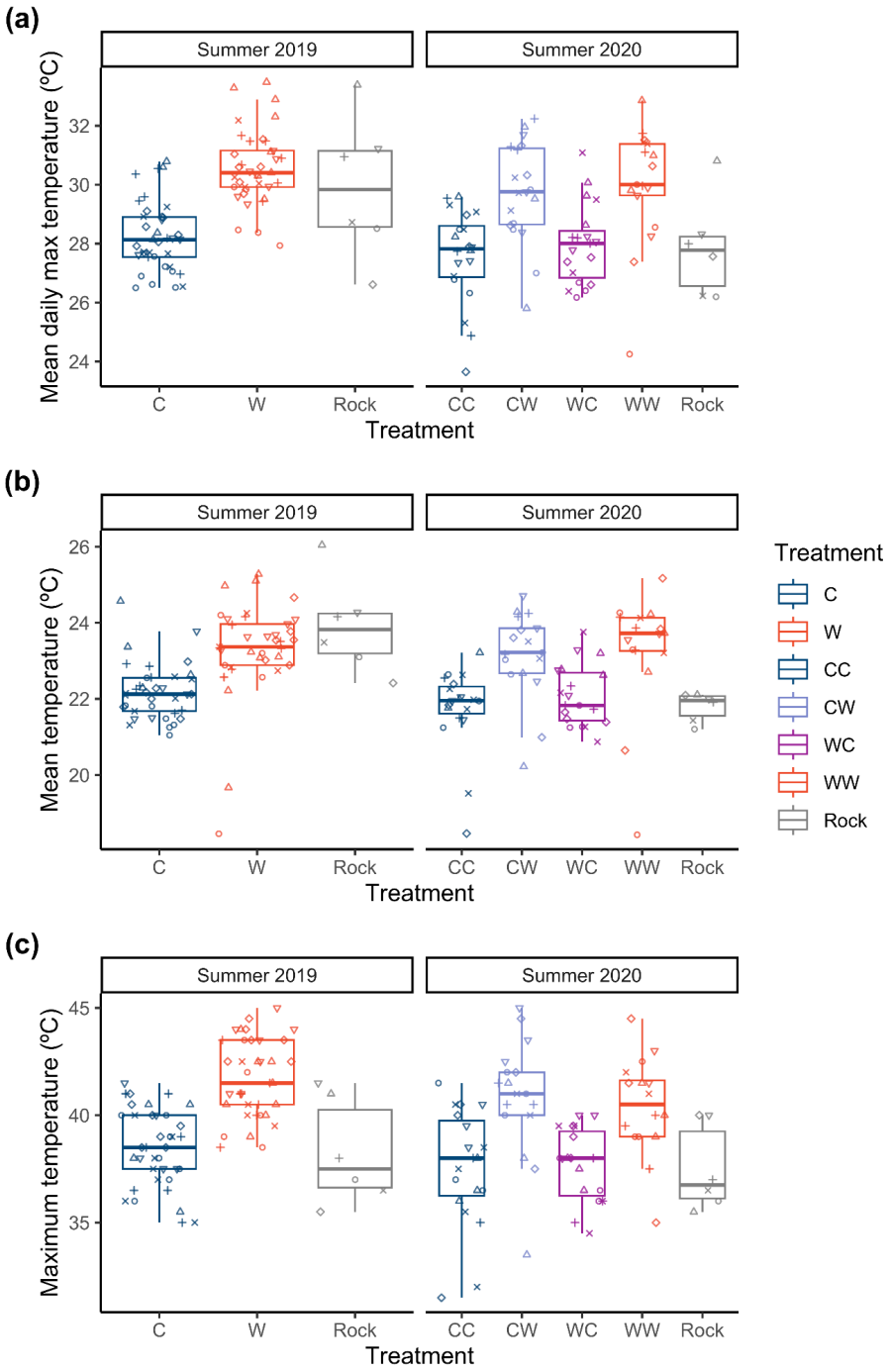

Figure S5. Differences in **(a)** mean daily maximum and **(b)** mean substratum temperatures during daytime summer low tides, and **(c)** absolute maximum temperatures of experimental tiles and adjacent bedrock recorded by temperature loggers at TESNO, EN. Points represent the mean value for each of the six experimental blocks, using only temperatures collected during daytime summer low tides between 1 June – 31 August. The exact number of temperature loggers recording data varied among treatments and over time. Treatment abbreviations as in Fig. S2.

Additional biological data

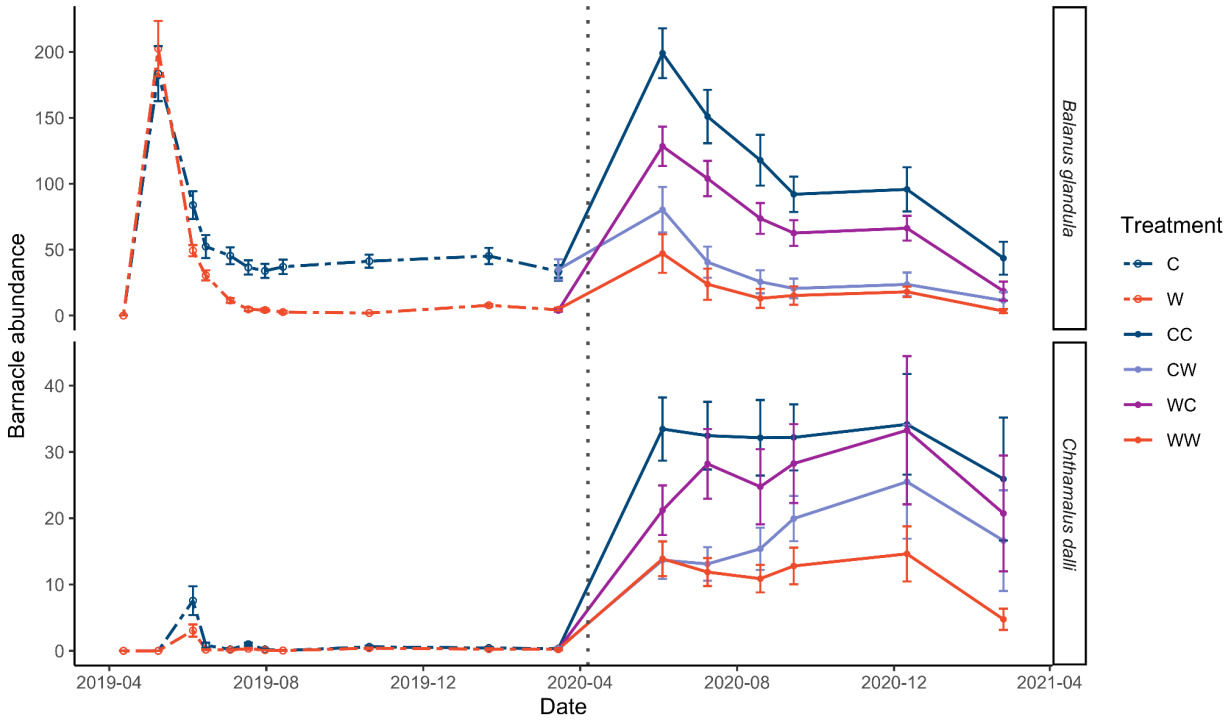

Figure S6. Mean abundance of *Balanus glandula* and *Chthamalus dalli* acorn barnacles on experimental tiles at TESNO, including recruits, over the course of the entire experiment. Error bars represent standard errors about the mean. The dotted line represents the time at which experimental treats were switched from those of Year 1 to Year 2. Note that y axes are on different scales. Treatment abbreviations as in Fig. S2.

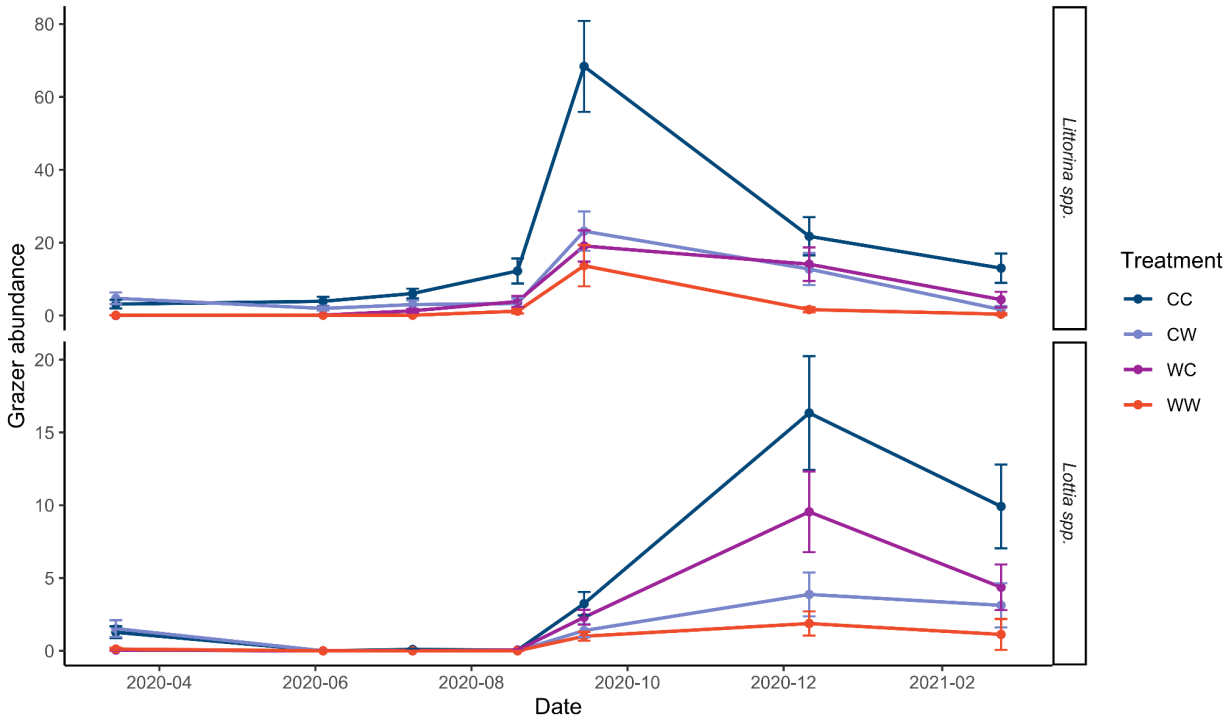

Figure S7. Mean abundance of *Lottia* spp. and *Littorina spp.* gastropod grazers on experimental tiles at TESNO, EN, including recruits, over the course of the entire experiment. Error bars represent standard errors about the mean. Note that y axes are on different scales. Treatment abbreviations as in Fig. S2.

Temporal patterns in invertebrate Shannon diversity mirrored patterns in overall species richness; diversity remained low in the first year, exhibited a peak in fall of the second year, and gradually declined thereafter (Fig. S8b). In the first year, the negative effect of warming on Shannon diversity was more apparent in late winter compared to post-summer (Fig. S9a; Type III ANOVA; $\chi^2_1 = 13.01$, $P < 0.001$). In the second year, invertebrate Shannon diversity was higher post-summer than during winter (Type III ANOVA; $\chi^2_1 = 41.80$, $P < 0.001$), and treatments that were warmed during the first year (WC and WW) had significantly lower Shannon diversity than their comparatively cool counterparts ($\chi^2_1 = 9.37$, $P = 0.00220$). Warming during the second year (CW and WW) exerted a negative, though marginally insignificant, effect on Shannon diversity (treatment_{y1}: $\chi^2_1 = 3.69$, $P = 0.0546$). Tukey-Kramer *post hoc* tests showed

that the successively warm treatment (WW) had substantially lower algal cover than the successively cool treatment (CC) and the warm–cool treatment (WC), but not the cool–warm treatment (CW).

Algal Shannon diversity was highest in winter, and cover became low and sometimes nonexistent from late summer to early fall (Fig. S8c). Where temperatures were cooler during the first year of the experiment, algal cover was higher (Fig. S9c), leading to a significant negative effect of warming (Type II ANOVA; $\chi^2 = 14.01$, $P < 0.001$). In the second year of the experiment, algal cover (and thus diversity) was negligible over the summer and was highly variable within treatment groups at the end of the winter. Warming, whether applied during the first or second year, did not exert a significant effect on algal Shannon diversity.

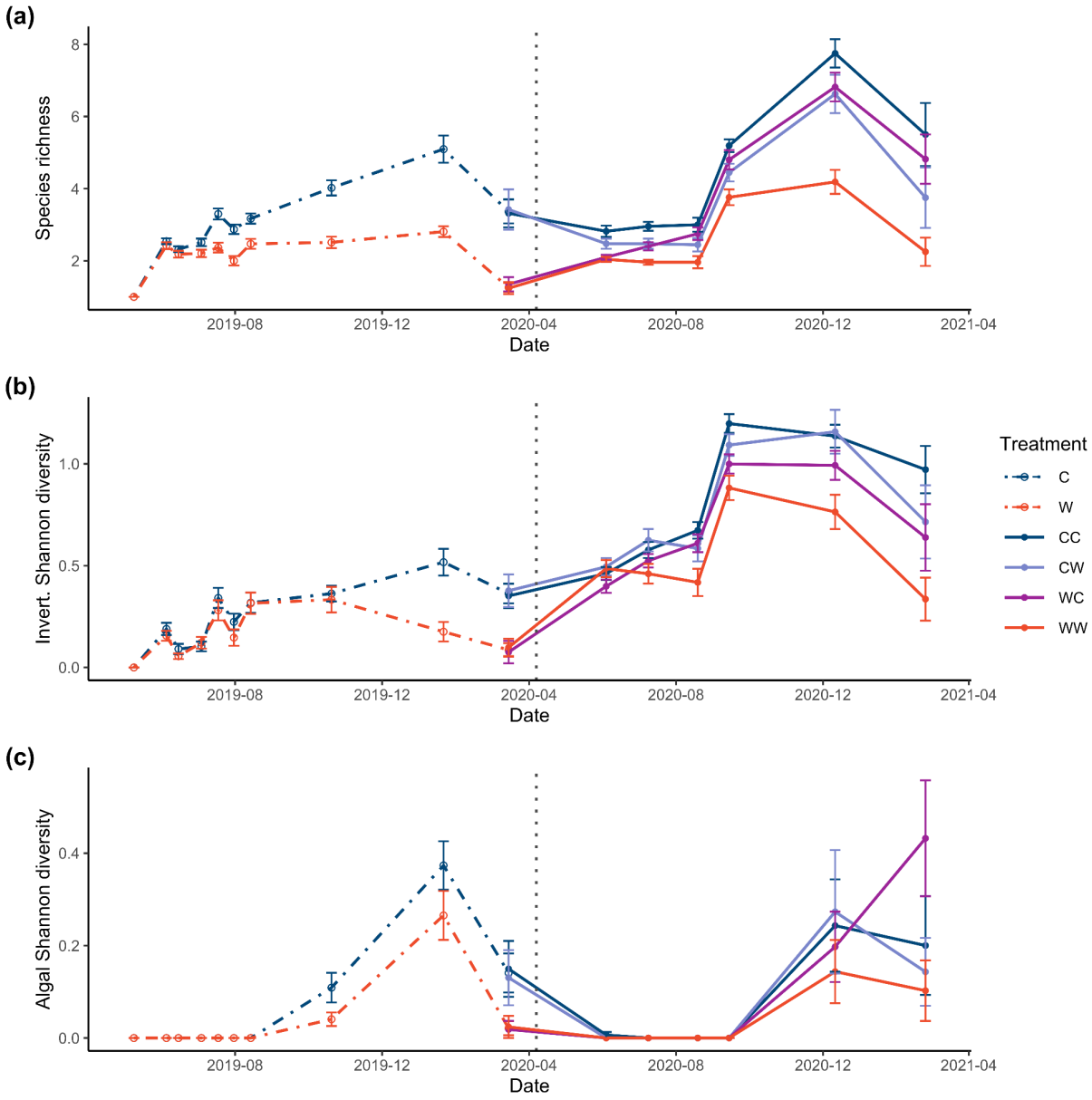

Figure S8. The effect of temperature treatments on alpha diversity of experimental communities over time, as described by changes in the **(a)** species richness of whole tile communities and Shannon diversity of **(b)** the invertebrate community and **(c)** the algal community. Error bars represent standard errors about the mean. The dotted vertical line represents the time at which experimental treatments were switched from those of Year 1 to Year 2. Note that y axes are on different scales. Treatment abbreviations as in Fig. S2.

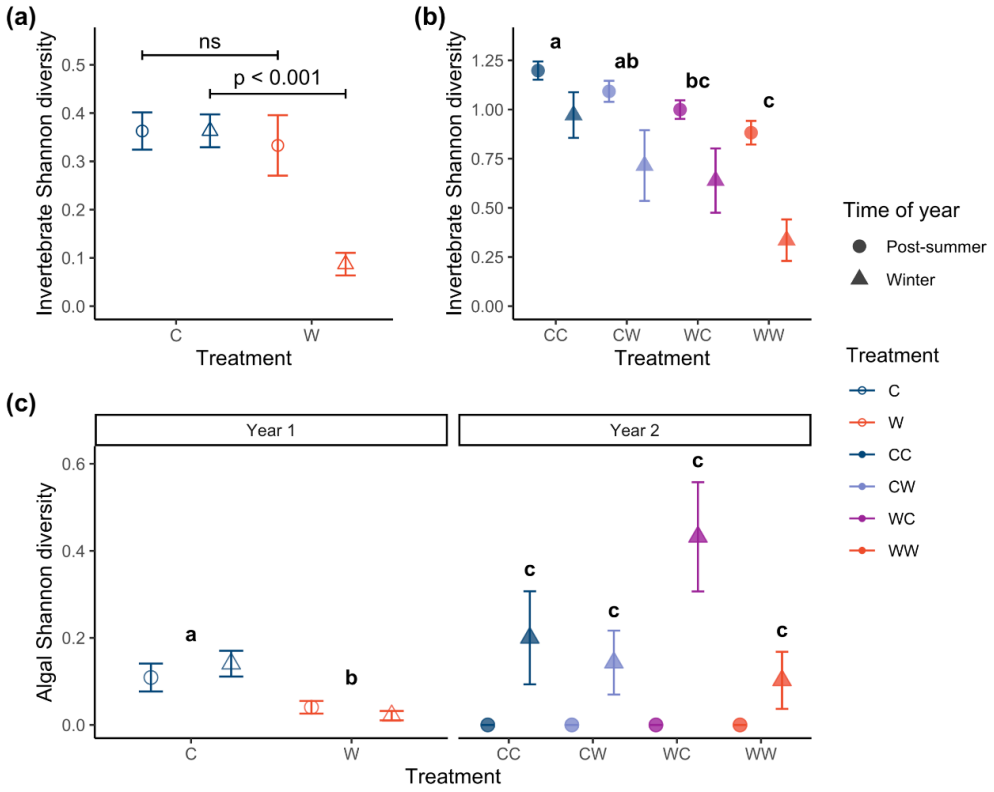

Figure S9. Shannon diversity of the **(a)** invertebrate community during the first year, **(b)** invertebrate community during the second year, and **(c)** algal community during the entire two-year passive warming experiment at TESNO, EN. Samples were obtained through visual surveys. Error bars represent standard error about the mean. Differences between treatment groups, as determined using Tukey-Kramer *post hoc* tests, are indicated through brackets (ns = non-significant) or lowercase letters. Treatment abbreviations as in Fig. S2.

The richness and Shannon diversity of destructively sampled tile epifaunal communities were also examined (Fig. S10). Richness was similar between sampling timepoints, but warming applied during the second summer had a negative effect on epifaunal richness (Type III ANOVA; $\chi^2_1 = 5.69$, $P = 0.0171$), while warming applied during the second summer had a persistent negative effect (treatment_{y1}: $\chi^2_1 = 3.91$, $P = 0.0480$). Trends in Shannon diversity were analogous; warming had both contemporaneous ($\chi^2_1 = 15.49$, $P = 0.001$), and persistent negative effects on the Shannon diversity of the epifaunal community (treatment_{y1}: $\chi^2_1 = 12.87$, $P = 0.001$).

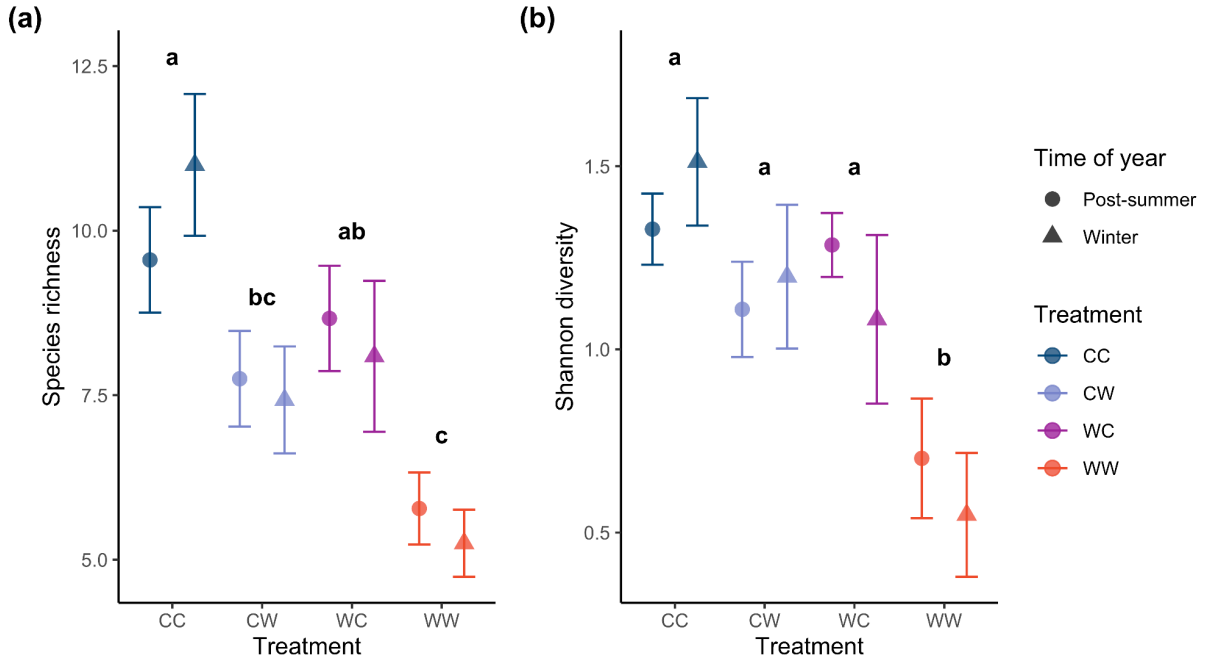

Figure S10. (a) Species richness and **(b)** Shannon diversity of epifaunal community within destructively sampled experimental tiles in the second year of a multi-year passive warming experiment at TESNO, EN. Error bars represent standard error about the mean. Differences between treatment groups, as determined using Tukey-Kramer *post hoc* tests, are indicated using lowercase letters. Treatment abbreviations as in Fig. S2.

Changes in community structure were plotted through time to examine qualitative patterns of change through community trajectory analysis in the *ecotraj* package (version 0.0.1; De Cáceres et al. 2019). To do this, the 'average' community structure of each treatment group at each timepoint, using abundance and cover data from visual surveys, was determined by averaging species abundance or cover for all experimental tiles in each treatment, and distance-based redundancy analysis was performed on these averaged communities for all timepoints with 999 random starts and autotransformation of data using Bray-Curtis distances.

Differences in the temperature of tile treatments drove divergences in the biological community inhabiting these tiles over time (Fig. S10). Cool and warm treatments quickly diverged in composition over the first summer, and this divergence grew through the winter.

Communities followed a similar trajectory during the first part of the second summer. However, treatment differences were apparent by the end of the summer, with CC and WC treatments grouping together and WW and CW treatments grouping together. Following the second winter, the WW and CC treatments were quite similar in composition to the warm and cool treatments, respectively, at the same time the previous year, while the CW and WC treatments were intermediate in their composition.

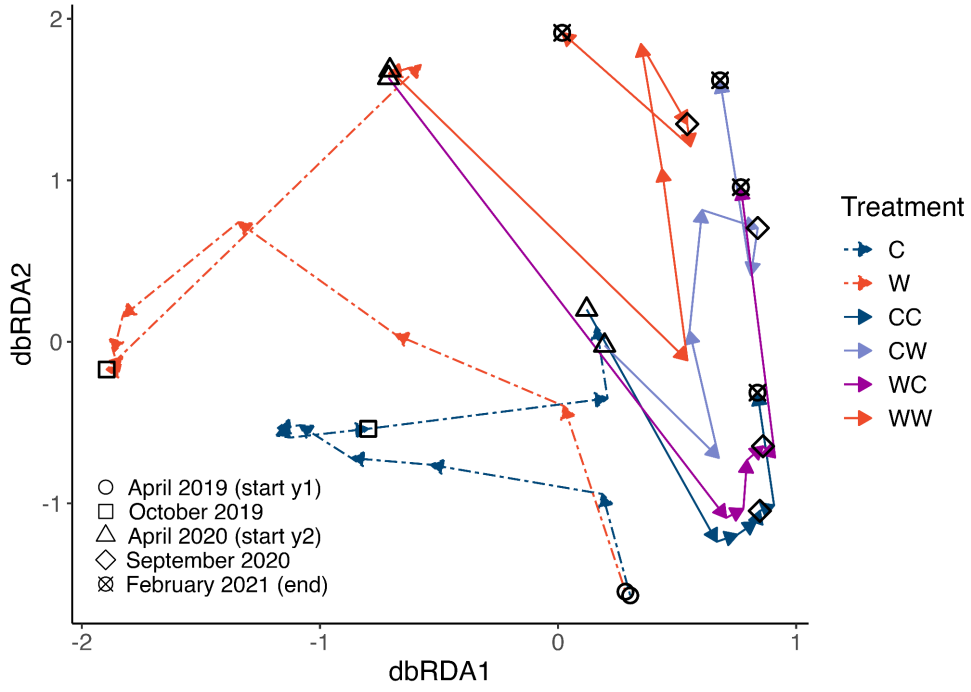

Figure S10. Trajectory plot for experimental tile communities over the course of the experiment from April 2019 to February 2021. Trajectories represent the 'average' community — calculated by averaging the abundance of each species across experimental tile units in each treatment at each timepoint — with the start and end terminus of each arrow based on Bray-Curtis dissimilarities among communities. The direction of arrows shows the flow of time from the beginning to the end of the experiment, and the length of each arrow correlates with the magnitude of community shift between timepoints. Different points along each treatment trajectory help visually identify key timepoints during the experiment (experiment start, end of summer in y1=year one, start of y2=year two, end of summer in y2, experiment end). Sample sizes for each treatment group changes through time. See Fig. S2 for treatment abbreviations.

Epifaunal communities

Table S3. Inventory of epifaunal taxa found during destructive surveys of intertidal barnacle bed communities on experimental tiles at TESNO, EN.

Taxon name	Authority
Amiphopoda	Latreille, 1816
Anthopleura elegantissima	Brandt, 1835
Annelida	
Arachnida	
Cyprid larva	Burmeister, 1834
Copepoda	Milne Edwards, 1840
Dynamenella sheareri	Hatch, 1947
Emplectonema gracile	Johnston, 1837
Hymenoptera	
Insecta	
Isopoda	Latreille, 1817
Lasaea rubra	Montagu, 1803
Littorina scutulata	Gould, 1849
Littorina sitkana	Philippi, 1846
Lottia digitalis	Rathke, 1833
Lottia paradigitalis	Fritchman, 1960
Lottia pelta	Rathke, 1833
Lottia scutum	Rathke, 1833
Lottia sp.	Gray, 1833
Mytilus sp.	Linnaeus, 1758
Neostylidium eschrichtii	Middendorff, 1849
Nemertea	
Oedoparena sp.	Curran, 1934
Onchidoris bilamellata	Linnaeus, 1767
Pagurus hirsutiusculus	Dana, 1851
Platyhelminthes	Minot, 1876
Polychaeta	Grube, 1850
Polychaeta	Grube, 1850
Sabellidae	Latreille, 1825
Syllidae	Grube, 1850

REFERENCES

De Cáceres, M., Coll, L., Legendre, P., Allen, R., Wiser, S., Fortin, M., Condit, R., and Hubbell, S. 2019. Trajectory analysis in community ecology. Ecological Monographs **89**: e01350.

Fisheries and Oceans Canada. 2022. Tides, currents, and water levels. https://tides.gc.ca/en.

APPENDIX S2: STATISTICAL OUTPUTS

The effect of single versus successive warm summers on an intertidal community

Amelia V. Hesketh, Cassandra A. Konecny, Sandra M. Emry, Christopher D. G. Harley

Analysis 1: Substratum temperature

Model S1

Residual maximum daily temperature ~ treatment + (1|block/number)

Table S4. Model summary table for Model S1, a linear mixed effects model testing the effect of treatment on residual maximum daily temperature recorded by temperature loggers in the first year of the passive warming experiment. Coefficients given are relative to the cool treatment, and the model was tested using a Type I ANOVA. SE = standard error, df = degrees freedom.

Term	Coefficient	SE	Sum Sq.	*F*	df (numerator)	df (denominator)	*P*
Intercept	-1.204	0.426					
Treatment–Rock	1.934	0.450	414.5	44.88	2	72.37	**2.11×10^{-13}**
Treatment–Warm	2.220	0.239					

Table S5. Tukey-Kramer *post hoc* comparison of the residual maximum daily temperatures within treatment groups in year one of the passive warming experiment. SE = standard error, C = cool treatment, W = warm treatment

Contrast	Estimate	SE	*z* ratio	*P*
C–Rock	-1.934	0.450	-4.30	**0.0001**
C–W	-2.220	0.239	-9.28	**<0.0001**
Rock–W	-0.285	0.450	-0.63	0.802

Table S6. Model summary table for Model S1, a linear mixed effects model testing the effect of treatment on the residual maximum daily temperature recorded by temperature loggers in the second year of the experiment. Coefficients given are relative to the cool summer – cool summer (CC) treatment, and the model was tested using a Type I ANOVA. SE = standard error, df = degrees freedom. CW = cool summer – warm summer, WC = warm summer – warm summer, WW = warm summer – warm summer.

Term	Coefficient	SE	Sum Sq.	*F*	df (numerator)	df (denominator)	*P*
Intercept	-1.078	0.392					
Treatment–CW	2.222	0.348					
Treatment–Rock	1.155	0.500	291.7	21.00	4	68.75	$\mathbf{2.45 \cdot 10^{-11}}$
Treatment–WC	0.076	0.342					
Treatment–WW	2.438	0.357					

Table S7 Tukey-Kramer *post hoc* comparison of the residual maximum daily temperature of treatment groups in year two of the passive warming experiment. See Table S5 for treatment codes and abbreviations.

Contrast	Estimate	SE	*z* ratio	*P*
CC–CW	-2.222	0.348	-6.38	**<0.0001**
CC–Rock	-1.155	0.500	-2.31	0.141
CC-WC	-0.076	0.342	-0.22	1.000
CC–WW	-2.438	0.357	-6.83	**<0.0001**
CW–Rock	1.067	0.504	2.12	0.213
CW–WC	2.147	0.349	6.15	**<0.0001**
CW–WW	-0.216	0.362	-0.60	0.975
Rock–WC	1.080	0.500	2.16	0.196
Rock–WW	-1.283	0.510	-2.52	0.0869
WC–WW	-2.363	0.358	-6.61	**<0.0001**

Model S2

Maximum daily temperature ~ treatment + (1|block/number) + (1|date)
Family: Gaussian

Table S8. Model summary table for Model S2, a linear mixed effects model testing the effect of treatment on the maximum daily temperature recorded by temperature loggers in the first year of the passive warming experiment. Coefficients given are relative to the cool treatment, and the model was tested using a Type I ANOVA. SE = standard error, df = degrees freedom.

Term	Coefficient	SE	Sum Sq.	*F*	df (numerator)	df (denominator)	*P*
Intercept	28.22	0.799					
Treatment–Rock	1.944	0.450	421.36	45.04	2	72.41	**$1.96 \cdot 10^{-13}$**
Treatment–Warm	2.222	0.239					

Table S9. Tukey-Kramer *post hoc* comparison of the maximum daily temperatures within treatment groups in year one of the passive warming experiment. SE = standard error, C = cool treatment, W = warm treatment

Contrast	Estimate	SE	*z* ratio	*P*
C–Rock	-1.944	0.450	-4.32	**<0.0001**
C–W	-2.222	0.239	-9.29	**<0.0001**
Rock–W	-0.277	0.450	-0.616	0.811

Table S10. Model summary table for Model S2, a linear mixed effects model testing the effect of treatment on the maximum daily temperature recorded by temperature loggers in the second year of the experiment. Coefficients given are relative to the cool summer – cool summer (CC) treatment, and the model was tested using a Type I ANOVA. SE = standard error, df = degrees freedom. See Table S6 for abbreviations.

Term	Coefficient	SE	Sum Sq.	*F*	df (numerator)	df (denominator)	*P*
Intercept	27.96	0.722					
Treatment–CW	2.224	0.348					
Treatment–Rock	1.140	0.500	295.4	20.96	4	73.85	**$2.54 \cdot 10^{-11}$**
Treatment–WC	0.076	0.342					
Treatment–WW	2.438	0.357					

Table S11. Tukey-Kramer *post hoc* comparison of the maximum daily temperature of treatment groups in year two of the passive warming experiment. See Table S6 for treatment codes and abbreviations.

Contrast	Estimate	SE	*z* ratio	*P*
CC–CW	-2.224	0.348	-6.38	**<0.0001**
CC–Rock	-1.140	0.500	-2.28	0.152
CC-WC	-0.077	0.342	-0.22	0.999
CC–WW	-2.438	0.357	-6.82	**<0.0001**
CW–Rock	1.084	0.505	2.15	0.200
CW–WC	2.148	0.349	6.15	**<0.0001**
CW–WW	-0.214	0.362	-0.59	0.976
Rock–WC	1.064	0.501	2.12	0.211
Rock–WW	-1.298	0.510	-2.54	0.0814
WC–WW	-2.362	0.358	-6.60	**<0.0001**

Model S3

Mean daily temperature ~ treatment + (1|block/number) + (1|date)
Family: Gaussian

Table S12. Model summary table for Model S3, a linear mixed effects model testing the effect of treatment on the mean daily temperature of experimental tiles in the first year of the passive warming experiment. Coefficients given are relative to the cool treatment, and the model was tested using a Type I ANOVA. df = degrees of freedom, SE = standard error.

Term	Coefficient	SE	Sum Sq.	*F*	df (numerator)	df (denominator)	*P*
Intercept	22.12	0.513					
Treatment–Rock	1.912	0.297					
Treatment–Warm	1.342	0.158	158.5	45.53	2	79.25	**1.45×10^{-13}**

Table S13. Tukey-Kramer *post hoc* comparison of the maximum daily temperature of treatment groups in year one of the passive warming experiment. SE = standard error, C = cool treatment, W = warm treatment

Contrast	Estimate	SE	*z* ratio	*P*
C–Rock	-1.912	0.297	-6.43	**<0.0001**
C–W	-1.342	0.158	-8.50	**<0.0001**
Rock–W	0.570	0.297	1.92	0.134

Table S14. Model summary table for Model S3, a linear mixed effects model testing the effect of temperature treatment on the mean daily temperature of experimental tiles in the second year of the experiment. Coefficients given are relative to the cool summer – cool summer (CC) treatment, and the model was tested using a Type I ANOVA. See Table S6 for abbreviations.

Term	Coefficient	SE	Sum Sq.	F	df (numerator)	df (denominator)	*P*
Intercept	21.800	0.509					
Treatment–CW	1.289	0.209					
Treatment–Rock	1.128	0.301	134.9	21.17	4	67.89	**2.30×10^{-11}**
Treatment–WC	0.132	0.205					
Treatment–WW	1.548	0.214					

Table S15. Tukey-Kramer *post hoc* comparison of mean daily temperature of treatment groups in year two of the passive warming experiment. See Table S6 for treatment codes and abbreviations.

Contrast	Estimate	SE	*z* ratio	*P*
CC–CW	-1.288	0.209	-6.16	**<0.0001**
CC–Rock	-1.126	0.301	-3.75	**0.0017**
CC-WC	-0.132	0.205	-0.64	0.968
CC–WW	-1.548	0.214	-7.22	**<0.0001**
CW–Rock	0.161	0.304	0.530	0.984
CW–WC	1.156	0.210	5.51	**<0.0001**
CW–WW	-0.259	0.218	-1.19	0.757
Rock–WC	0.996	0.301	3.30	**0.00850**
Rock–WW	-0.420	0.307	1.37	0.648
WC–WW	-1.416	0.215	-6.59	**<0.0001**

Model S4

Maximum temperature ~ treatment + (1|block)
Family: Gaussian

Table S16. Model summary table for Model S4, a linear mixed effects model testing the effect of treatment on the maximum temperature of experimental tiles in the first year of the passive warming experiment. Coefficients given are relative to the cool treatment, and the model was tested using a Type I ANOVA. SE = standard error, df = degrees of freedom

Term	Coefficient	SE	Sum Sq.	*F*	df (numerator)	df (denominator)	*P*
Intercept	38.5	0.4					
Treatment–Rock	-0.3	0.8					
Treatment–Warm	3.1	0.4	194.68	33.46	2	72.62	**5.01×10^{-11}**

Table S17. Tukey-Kramer *post hoc* comparison of the maximum temperature of treatment groups in year one of the passive warming experiment. SE = standard error, C = cool treatment, W = warm treatment, df = degrees of freedom

Contrast	Estimate	SE	df	*t* ratio	*P*
C–Rock	0.27	0.75	72.1	0.36	0.931
C–W	-3.13	0.40	73.3	-7.75	**<0.0001**
Rock–W	-3.40	0.75	72.1	-4.52	**0.0001**

Table S18. Model summary table for Model S4, a linear mixed effects model testing the effect of treatment on the maximum temperature of experimental tiles in the second year of the experiment. Coefficients given are relative to the cool summer – cool summer (CC) treatment, and the model was tested using a Type I ANOVA. See Table S6 for abbreviations.

Term	Coefficient	SE	Sum Sq.	F	df (numerator)	df (denominator)	*P*
Intercept	37.5	0.7					
Treatment–CW	3.3	0.7					
Treatment–Rock	-0.02	1.0	178.3	9.36	4	67.15	**4.50×10^{-6}**
Treatment–WC	0.2	0.7					
Treatment–WW	3.0	0.7					

Table S19. Tukey-Kramer *post hoc* comparison of the maximum temperature of treatment groups in year two of the passive warming experiment. See Table S6 for treatment codes and abbreviations.

Contrast	Estimate	SE	df	*t* ratio	*P*
CC–CW	-3.323	0.735	67.6	-4.52	**0.0002**
CC–Rock	0.016	1.024	67.2	0.016	1.00
CC-WC	-0.154	0.709	67.2	-0.22	1.00
CC–WW	-2.971	0.747	67.7	-3.97	**0.0016**
CW–Rock	3.339	0.411	67.0	3.22	**0.0163**
CW–WC	3.169	0.731	67.2	4.34	**0.0005**
CW–WW	0.352	0.761	67.1	0.46	0.990
Rock–WC	-0.170	1.022	67.0	-0.17	1.00
Rock–WW	-2.987	1.045	67.1	-2.86	**0.0436**
WC–WW	-2.817	0.743	67.3	-3.79	**0.0029**

Model S5

Balanus glandula recruit year 1 abundance ~ treatment_{y1} + (1|block)
Family: Quasi-Poisson

Table S20. Model summary table for Model S5, a generalized linear mixed effects model of *B. glandula* recruit abundance on experimental tiles during peak recruitment in the first year of the passive warming experiment. Coefficients given are relative to the cool treatment, and the model was tested using a Type II ANOVA. Treatment_{y1} = treatment in year one, SE = standard error, df = degrees of freedom

Term	Coefficient	SE	χ^2	df	*P*
Intercept	4.984	0.326			
Treatment_{y1}	0.0899	0.0769	1.37	1	0.243

Model S6

Balanus glandula recruit year 2 abundance ~ $treatment_{y1}$ * $treatment_{y2}$ + (1|block)
Family: Quasi-Poisson

Table S21. Model summary table for Model S6, a generalized linear mixed effects model of *B. glandula* recruit abundance on experimental tiles during peak recruitment in the first year of the passive warming experiment. Coefficients given are relative to the cool treatment, and the model was tested using a Type III ANOVA. $Treatment_{y1}$ = treatment in year one, $treatment_{y2}$ = treatment in year two, SE = standard error, df = degrees of freedom

Term	Coefficient	SE	χ^2	df	*P*
Intercept	4.934	0.159			
$Treatment_{y1}$	-0.3884	0.1576	6.07	1	**0.0138**
$Treatment_{y2}$	-1.301	0.210	38.34	1	**$5.94x10^{-10}$**
$Treatment_{y1}$ * $Treatment_{y2}$	0.3537	0.2900	1.49	1	0.223

Table S22. Tukey-Kramer *post hoc* comparison of *B. glandula* recruitment between treatment groups in year two of the passive warming experiment. See Table S6 for treatment codes and abbreviations.

Contrast	Estimate	SE	df	*z* ratio	*P*
CC–WC	0.388	0.158	Inf	2.46	0.0657
CC–CW	1.301	0.210	Inf	6.19	**<0.0001**
CC–WW	1.335	0.193	Inf	6.91	**<0.0001**
WC–CW	0.912	0.220	Inf	4.15	**0.0002**
WC–WW	0.947	0.206	Inf	4.60	**<0.0001**
CW–WW	0.035	0.242	Inf	0.14	0.999

Model S7

Chthamalus dalli recruit year 1 abundance ~ treatment_{y1} + (1|block)
Family: Quasi-Poisson

Table S23. Model summary table for Model S7, a generalized linear mixed effects model of *C. dalli* recruit abundance on experimental tiles during peak recruitment in the first year of the passive warming experiment. Coefficients given are relative to the cool treatment, and the model was tested using a Type II ANOVA. See Table S21 for abbreviations.

Term	Coefficient	SE	χ^2	df	*P*
Intercept	1.692	0.303			
Treatment_{y1}	-0.469	0.231	4.13	1	**0.0422**

Model S8

Chthamalus dalli recruit year 2 abundance ~ treatment_{y1} * treatment_{y2} + (1|block)
Family: Quasi-Poisson

Table S24. Model summary table for Model S8, a generalized linear mixed effects model of *B. glandula* recruit abundance on experimental tiles during peak recruitment in the first year of the passive warming experiment. Coefficients given are relative to the cool treatment, and the model was tested using a Type III ANOVA. See Table S21 for abbreviations.

Term	Coefficient	SE	χ^2	df	*P*
Intercept	3.347	0.208			
Treatment_{y1}	-0.392	0.166	5.56	1	**0.0184**
Treatment_{y2}	-0.852	0.195	19.16	1	**1.20×10^{-5}**
Treatment_{y1} * Treatment_{y2}	0.430	0.272	2.50	1	0.114

Table S25. Tukey-Kramer *post hoc* comparison of *C. dalli* recruitment between treatment groups in year two of the passive warming experiment. See Table S6 for treatment codes and abbreviations.

Contrast	Estimate	SE	df	*z* ratio	*P*
CC–WC	0.392	0.158	Inf	2.36	0.0856
CC–CW	0.852	0.195	Inf	4.38	**0.0001**
CC–WW	0.815	0.178	Inf	4.58	**<0.0001**
WC–CW	0.460	0.208	Inf	2.22	0.119
WC–WW	0.423	0.192	Inf	2.20	0.124
CW–WW	-0.038	0.215	Inf	-0.18	0.998

Model S9

Balanus glandula year 1 adult abundance ~ $treatment_{y1}$ + (1|block)
Family: Quasi-Poisson

Table S26. Model summary table for Model S9, a generalized linear mixed effects model of adult *B. glandula* abundance on experimental tiles at the end of the first year of the passive warming experiment. Coefficients given are relative to the cool treatment, and the model was tested using a Type II ANOVA. See Table S21 for abbreviations.

Term	Coefficient	SE	χ^2	df	*P*
Intercept	3.237	0.275			
$Treatment_{y1}$	-1.524	0.148	106.20	1	**$<2.2 \times 10^{-16}$**

Model S10

Balanus glandula year 2 adult abundance ~ $treatment_{y1}$ * $treatment_{y2}$ + (1|block)
Family: Quasi-Poisson

Table S27. Model summary table for Model S10, a generalized linear mixed effects model of adult *B. glandula* abundance on experimental tiles at the end of the second year of the passive warming experiment. Coefficients given are relative to the cool treatment, and the model was tested using a Type III ANOVA. See Table S21 for abbreviations.

Term	Coefficient	SE	χ^2	df	*P*
Intercept	3.487	0.379			
$Treatment_{y1}$	-0.822	0.477	2.97	1	0.0846
$Treatment_{y2}$	-0.807	0.505	2.55	1	0.110
$Treatment_{y1}$ * $Treatment_{y2}$	0.156	0.715	0.048	1	0.827

Table S28. Tukey-Kramer *post hoc* comparison of adult *B. glandula* abundance between treatment groups in year two of the passive warming experiment. See Table S6 for treatment codes and abbreviations.

Contrast	Estimate	SE	df	*z* ratio	*P*
CC–WC	0.822	0.477	Inf	1.73	0.311
CC–CW	0.807	0.505	Inf	1.60	0.380
CC–WW	1.473	0.478	Inf	3.08	**0.0111**
WC–CW	-0.016	0.551	Inf	-0.028	1.00
WC–WW	0.651	0.525	Inf	1.24	0.601
CW–WW	0.666	0.535	Inf	1.25	0.598

Model S11

Chthamalus dalli year 1 adult abundance ~ treatment_{y1} + (1|block)
Family: Quasi-Poisson

Table S29. Model summary table for Model S11, a generalized linear mixed effects model of adult *C. dalli* abundance on experimental tiles at the end of the first year of the passive warming experiment. Coefficients given are relative to the cool treatment, and the model was tested using a Type II ANOVA. See Table S21 for abbreviations.

Term	Coefficient	SE	χ^2	df	*P*
Intercept	-1.654	0.572			
Treatment_{y1}	-0.287	0.356	0.65	1	0.420

Model S12

Chthamalus dalli year 2 adult abundance ~ $treatment_{y1}$ * $treatment_{y2}$ + (1|block)
Family: Quasi-Poisson

Table S30. Model summary table for Model S12, a generalized linear mixed effects model of adult *C. dalli* abundance on experimental tiles at the end of the second year of the passive warming experiment. Coefficients given are relative to the cool treatment, and the model was tested using a Type III ANOVA. See Table S21 for abbreviations.

Term	Coefficient	SE	χ^2	df	*P*
Intercept	3.080	0.408			
$Treatment_{y1}$	-0.502	0.462	1.18	1	0.277
$Treatment_{y2}$	-0.239	0.490	0.24	1	0.626
$Treatment_{y1}$ * $Treatment_{y2}$	-0.139	0.685	0.041	1	0.840

Table S31. Tukey-Kramer *post hoc* comparison of adult *C. dalli* abundance between treatment groups in year two of the passive warming experiment. See Table S6 for treatment codes and abbreviations.

Contrast	Estimate	SE	df	*z* ratio	*P*
CC–WC	0.502	0.462	Inf	1.09	0.698
CC–CW	0.239	0.490	Inf	0.49	0.962
CC–WW	0.879	0.450	Inf	1.95	0.207
WC–CW	-0.263	0.518	Inf	-0.51	0.957
WC–WW	0.377	0.487	Inf	0.77	0.866
CW–WW	0.641	0.500	Inf	1.28	0.575

Model S13

Lottia spp. abundance ~ treatment_{y1} * treatment_{y2} + date + (1|block)
Family: Quasi-Poisson

Table S32. Model summary table for Model S13, a generalized linear mixed effects model of *Lottia* spp. abundance on experimental tiles. Data were collected at the end of the second summer and in late winter, on 14 September 2020 and 21 February 2021. Coefficients for treatment are given are relative to the cool treatment, and the model was tested using a Type III ANOVA. See Table S21 for abbreviations.

Term	Coefficient	SE	χ^2	df	*P*
Intercept	0.758	0.507			
Treatment_{y1}	-0.413	0.204	4.10	1	**0.0428**
Treatment_{y2}	-0.747	0.268	7.75	1	**0.00537**
Date	0.794	0.181	19.21	1	**1.17×10^{-5}**
Treatment_{y1} * Treatment_{y2}	-0.348	0.409	0.72	1	0.395

Table S33. Tukey-Kramer *post hoc* comparison of *Lottia* spp. abundance between treatment groups in year two of the passive warming experiment. See Table S6 for treatment codes and abbreviations.

Contrast	Estimate	SE	df	*z* ratio	*P*
CC–WC	0.413	0.204	Inf	2.03	0.179
CC–CW	0.747	0.268	Inf	2.78	**0.0275**
CC–WW	1.507	0.301	Inf	5.02	**<0.0001**
WC–CW	0.334	0.285	Inf	1.17	0.644
WC–WW	1.094	0.314	Inf	3.48	**0.00280**
CW–WW	0.760	0.355	Inf	2.14	0.140

Model S24

Littorina spp. abundance ~ treatment_{y1} * treatment_{y2} + date + (1|block)
Family: Quasi-Poisson

Table S34. Model summary table for Model S14, a generalized linear mixed effects model of *Littorina* spp. abundance on experimental tiles. Data were collected at the end of the second summer and in late winter, on 14 September 2020 and 21 February 2021. Coefficients given are relative to the cool treatment, and the model was tested using a Type III ANOVA. See Table S21 for abbreviations.

Term	Coefficient	SE	χ^2	df	*P*
Intercept	4.096	0.200			
Treatment_{y1}	-1.044	0.219	22.82	1	**1.78×10^{-6}**
Treatment_{y2}	-0.976	0.224	18.97	1	**1.33×10^{-5}**
Date	-1.608	0.228	49.65	1	**1.84×10^{-12}**
Treatment_{y1} * Treatment_{y2}	0.377	0.343	1.21	1	0.272

Table S35. Tukey-Kramer *post hoc* comparison of *Littorina* spp. abundance between treatment groups in year two of the passive warming experiment. See Table S6 for treatment codes and abbreviations.

Contrast	Estimate	SE	df	*z* ratio	*P*
CC–WC	1.044	0.219	Inf	4.78	**<0.0001**
CC–CW	0.976	0.224	Inf	4.36	**0.0001**
CC–WW	1.644	0.238	Inf	6.91	**<0.0001**
WC–CW	-0.068	0.253	Inf	-0.28	0.993
WC–WW	0.600	0.261	Inf	2.30	0.0982
CW–WW	0.667	0.269	Inf	2.48	0.0624

Model S15

Algal cover ~ treatment + s(time) + s(time, by = treatment) + s(block, type = "re")

Family: Gaussian

Table S36. Model summary table for Model S15, a generalized additive mixed model of differences in algal cover over time between treatments in the first year of the experiment. Estimates and differences between smooth functions are given relative to the cool treatment. See Table S6 for abbreviations.

Component	Term	Estimate	SE	t	*P*
Parametric	Intercept	32.613	1.989	16.40	**$<2x10^{-16}$**
	Treatment: W	-1.097	1.380	-0.80	0.427
		Effective df		**F**	***P***
Smooth	s(time)	7.47		98.97	**$<2x10^{-16}$**
	s(time):W	5.90		12.61	**$<2x10^{-16}$**
	s(block)	4.30		6.41	**$1.45x10^{-6}$**

Table S37. Model summary table for Model S15, a generalized additive mixed model of differences in algal cover over time between treatments in the second year of the experiment. Estimates and differences between smooth functions are given relative to the cool treatment. k=5 for smoothing functions of time. See Table S6 for abbreviations.

Component	Term	Estimate	SE	t	*P*
Parametric	Intercept	2.562	1.175	2.18	**0.0297**
	Treatment: CW	2.661	1.454	1.83	0.0678
	Treatment: WC	1.907	1.404	1.36	0.175
	Treatment: WW	0.120	1.330	0.091	0.928
		Effective df		**F**	***P***
Smooth	s(time)	3.92		20.83	**$<2x10^{-16}$**
	s(time):CW	2.36		2.87	0.108
	s(time):WC	1.82		7.47	**0.00593**
	s(time):WW	1.00		1.20	0.275
	s(block)	3.19		1.81	**0.0152**

Model S16

Species richness ~ $treatment_{y1}$ * date + (1|block)
Family: Poisson

Table S38. Model summary table for Model S18, a generalized linear mixed effects model of the species richness on experimental tile communities during the first year. Data were collected at the end of the summer, on 20 October 2019, and during the winter, on 15 March 2020. Coefficients given are relative to the cool treatment, and the model was tested using a Type III ANOVA. See Table S21 for abbreviations.

Term	Coefficient	SE	χ^2	df	*P*
Intercept	1.342	0.140			
$Treatment_{y1}$	-0.457	0.115	15.52	1	**8.15×10^{-5}**
Date	-0.163	0.095	2.98	1	0.0845
$Treatment_{y1}$ * Date	-0.503	0.160	9.85	1	**0.00170**

Model S17

Species richness ~ $treatment_{y1}$ * $treatment_{y2}$ + date + (1|block)
Family: Poisson

Table S39. Model summary table for Model S19, a generalized linear mixed effects model of the species richness of experimental tiles during the second year. Data were collected at the end of the summer, on 14 September 2020, and during winter, on 24 February 2021. Coefficients given are relative to the cool treatment, and the model was tested using a Type III ANOVA. See Table S21 for abbreviations.

Term	Coefficient	SE	χ^2	df	*P*
Intercept	1.696	0.097			
$Treatment_{y1}$	-0.093	0.112	0.70	1	0.403
$Treatment_{y2}$	-0.221	0.123	3.25	1	0.0714
Date	-0.115	0.090	1.62	1	0.203
$Treatment_{y1}$ * $Treatment_{y2}$	-0.173	0.172	1.01	1	0.314

Table S40. Tukey-Kramer *post hoc* comparison of species richness between treatment groups in year two of the passive warming experiment. See Table S6 for treatment codes and abbreviations.

Contrast	Estimate	SE	df	*z* ratio	*P*
CC–WC	0.093	0.112	Inf	0.84	0.838
CC–CW	0.221	0.123	Inf	1.80	0.272
CC–WW	0.487	0.117	Inf	4.15	**2.00×10^{-4}**
WC–CW	0.128	0.121	Inf	1.01	0.742
WC–WW	0.394	0.121	Inf	3.26	**0.00620**
CW–WW	0.266	0.130	Inf	2.04	0.174

Model S20

Invertebrate Shannon diversity ~ $treatment_{y1}$ + date + (1|block)
Family: Tweedie
Dispersion formula: ~ $treatment_{y1}$

Table S41. Model summary table for Model S20, a generalized linear mixed effects model of the invertebrate Shannon diversity of experimental tile communities during the first year. Data were collected at the end of the summer, on 20 October 2019, and during winter, on 15 March 2020. Coefficients given are relative to the cool treatment, and the model was tested using a Type III ANOVA. See Table S21 for abbreviations.

Term	Coefficient	SE	χ^2	df	*P*
Intercept	-1.122	0.229			
$Treatment_{y1}$	-0.071	0.232	0.092	1	0.761
Date	-0.009	0.142	0.0039	1	0.950
$Treatment_{y1}$ * Date	-1.343	0.372	13.01	1	**3.09×10^{-4}**
Dispersion model					
Intercept	-1.435	0.089			
$Treatment_{y1}$	1.131	0.095			

Model S21

Invertebrate Shannon diversity ~ $treatment_{y1}$ * $treatment_{y2}$ + date + (1|block)
Family: Tweedie

Table S42. Model summary table for Model S21, a generalized linear mixed effects model of the invertebrate Shannon diversity of experimental tiles during the second year. Data were collected at the end of the summer, on 14 September 2020, and during the winter, on 24 February 2021 . Coefficients given are relative to the cool treatment, and the model was tested using a Type III ANOVA. See Table S21 for abbreviations.

Term	Coefficient	SE	χ^2	df	*P*
Intercept	1.254	0.070			
$Treatment_{y1}$	-0.246	0.080	9.37	1	**0.00220**
$Treatment_{y2}$	-0.163	0.085	3.69	1	0.0546
Date	-0.381	0.059	41.80	1	**1.01×10^{-10}**
$Treatment_{y1}$ * $Treatment_{y2}$	-0.017	0.114	0.022	1	0.883

Table S43. Tukey-Kramer *post hoc* comparison of invertebrate Shannon diversity between treatment groups in year two of the passive warming experiment. See Table S6 for treatment codes and abbreviations.

Contrast	Estimate	SE	df	*t* ratio	*P*
CC–WC	0.246	0.080	124	3.06	**0.0142**
CC–CW	0.163	0.085	124	1.92	0.224
CC–WW	0.425	0.076	124	5.60	**<0.0001**
WC–CW	-0.083	0.086	124	-0.97	0.766
WC–WW	0.179	0.077	124	2.33	0.0962
CW–WW	0.263	0.081	124	3.24	**0.0084**

Model S22

Algal Shannon diversity ~ $treatment_{y1}$ + date + (1|block)
Family: Tweedie

Table S44. Model summary table for Model S22, a generalized linear mixed effects model of the algal Shannon diversity of experimental tile communities. Data were collected at the end of the first summer following exposure to heat stress, on 20 October 2019. Coefficients given are relative to the cool treatment, and the model was tested using a Type II ANOVA. See Table S21 for abbreviations.

Term	Coefficient	SE	χ^2	df	*P*
Intercept	-2.444	0.490			
$Treatment_{y1}$	-1.341	0.358	14.01	1	**1.82×10^{-4}**
Date	-0.014	0.329	0.0018	1	0.966

Model S23

Algal Shannon diversity ~ $treatment_{y1}$ * $treatment_{y2}$ + (1|block)
Family: Tweedie

Table S45. Model summary table for Model S23, a generalized linear mixed effects model of the algal Shannon diversity of experimental tiles. Data were collected at the end of the first winter following recovery from heat stress, on 24 February 2021. Coefficients given are relative to the cool treatment, and the model was tested using a Type III ANOVA. See Table S21 for abbreviations.

Term	Coefficient	SE	χ^2	df	*P*
Intercept	-1.609	0.507			
$Treatment_{y1}$	0.7698	0.6407	1.444	1	0.230
$Treatment_{y2}$	-0.3348	0.8722	0.147	1	0.701
$Treatment_{y1}$ * $Treatment_{y2}$	-1.105	1.114	0.984	1	0.321

Table S46. Tukey-Kramer *post hoc* comparison of algal Shannon diversity between treatment groups in year two of the passive warming experiment. See Table S6 for treatment codes and abbreviations.

Contrast	Estimate	SE	df	z ratio	*P*
CC–WC	-0.770	0.641	Inf	-1.20	0.626
CC–CW	0.335	0.872	Inf	0.38	0.981
CC–WW	0.670	0.765	Inf	0.88	0.818
WC–CW	1.105	0.810	Inf	1.35	0.522
WC–WW	1.440	0.693	Inf	2.08	0.161
CW–WW	0.335	0.912	Inf	0.37	0.983

Model S24

Species assemblage ~ treatment

Table S47. Model summary table of PERMANOVA output for Model S24 describing differences in epifaunal community composition of experimental tiles destructively sampled on 14 September 2020. PERMANOVA uses constrained ordination via distance-based redundancy analyses with Bray-Curtis distances. df = degrees of freedom.

Term	df	Sum of squares	F	*P*
Treatment	3	1.145	1.495	0.0566
Residuals	31	7.913		

Table S48. Multiple pairwise comparisons of epifaunal community composition across treatments using constrained ordination via distance-based redundancy analyses with Bray-Curtis distances. Epifauna were destructively sampled on 14 September 2020. See Table S6 for treatment codes and abbreviations.

Comparison	df	Sum of squares	F	*P*
CC – CW	1	0.2726	1.164	0.277
CC – WC	1	0.2760	1.213	0.292
CC – WW	1	0.7796	2.705	**0.028**
CW – WC	1	0.04749	0.2157	0.985
CW – WW	1	0.4542	1.595	0.136
WC – WW	1	0.4386	1.595	0.134

Table S49. Model summary table of PERMANOVA output for Model S24 describing differences in epifaunal community composition of experimental tiles destructively sampled on 24 February 2021. PERMANOVA uses constrained ordination via distance-based redundancy analyses with Bray-Curtis distances. df = degrees of freedom.

Term	df	Sum of squares	F	*P*
Treatment	3	2.589	3.341	**0.0001**
Residuals	37	9.558		

Table S50. Multiple pairwise comparisons of epifaunal community composition across treatments using constrained ordination via distance-based redundancy analyses with Bray-Curtis distances. Epifauna were destructively sampled on 24 February 2021. See Table S6 for treatment codes and abbreviations.

Comparison	df	Sum of squares	F	*P*
CC – CW	1	0.9604	4.189	**0.009**
CC – WC	1	0.6442	2.448	**0.024**
CC – WW	1	1.757	6.833	**0.002**
CW – WC	1	0.1765	0.6794	0.702
CW – WW	1	0.4500	1.781	0.112
WC – WW	1	0.9809	3.497	**0.005**

Model S25

Species assemblage heterogeneity ~ treatment

Table S51. Model summary table of PERMDISP output for Model S25 of differences in epifaunal community composition heterogeneity of experimental tiles destructively sampled in September 2020. df = degrees of freedom.

Term	df	Sum of squares	Mean squares	F	*P*
Treatment	3	0.07327	0.02442	2.616	0.0686
Residuals	31	0.2894	0.0093		

Table S52. Model summary table of PERMDISP output for Model S25 of differences in epifaunal community composition heterogeneity of experimental tiles destructively sampled in February 2021. df = degrees of freedom.

Variable	df	Sum of squares	Mean squares	F	*P*
Treatment	3	0.03230	0.01077	0.5967	0.621
Residuals	37	0.6676	0.0180		

Model S26

Species richness ~ $treatment_{y1}$ * $treatment_{y2}$ + date
Family: Poisson

Table S53. Model summary table for Model S26, a generalized linear mixed effects model of the species richness of epifauna from destructively sampled tile communities collected on 14 September 2020 and 24 February 2021. Coefficients given are relative to the cool treatment, and the model was tested using a Type III ANOVA. See Table S6 for treatment codes and abbreviations.

Term	Coefficient	SE	χ^2	df	*P*
Intercept	2.303	0.099			
$Treatment_{y1}$	-0.2061	0.1042	3.910	1	**0.0480**
$Treatment_{y2}$	-0.2831	0.1187	5.686	1	**0.0171**
Date	0.0185	0.0834	0.0490	1	0.825
$Treatment_{y1}$ * $Treatment_{y2}$	-0.1233	0.1696	0.5283	1	0.467

Table S54. Tukey-Kramer *post hoc* comparison of species richness of epifauna from destructively sampled tile communities between treatment groups in year two of the passive warming experiment. See Table S6 for treatment codes and abbreviations.

Contrast	Estimate	SE	df	z ratio	*P*
CC–WC	0.206	0.104	Inf	1.98	0.197
CC–CW	0.283	0.119	Inf	2.39	**0.0800**
CC–WW	0.613	0.117	Inf	5.21	**<0.0001**
WC–CW	0.0771	0.123	Inf	0.628	0.923
WC–WW	0.406	0.122	Inf	3.33	**0.00480**
CW–WW	0.329	0.133	Inf	2.47	0.0645

Model S27
Shannon diversity ~ $treatment_{y1}$ * $treatment_{y2}$ + date
Family: Poisson

Table S55. Model summary table for Model S27, a generalized linear mixed effects model of the Shannon diversity of epifauna from destructively sampled tile communities collected on 14 September 2020 and 24 February 2021. Coefficients given are relative to the cool treatment, and the model was tested using a Type III ANOVA. See Table S6 for treatment codes and abbreviations.

Term	Coefficient	SE	χ^2	df	*P*
Intercept	1.404	0.148			
$Treatment_{y1}$	-0.2478	0.1441	2.957	1	0.0855
$Treatment_{y2}$	-0.2676	0.1578	2.880	1	0.0897
Date	0.0105	0.1074	0.0095	1	0.922
$Treatment_{y1}$ * $Treatment_{y2}$	-0.2753	0.2127	1.676	1	0.195

Table S56. Tukey-Kramer *post hoc* comparison of the Shannon diversity of epifauna from destructively sampled tile communities between treatment groups in year two of the passive warming experiment. See Table S6 for treatment codes and abbreviations.

Contrast	Estimate	SE	df	z ratio	*P*
CC–WC	0.248	0.144	69	1.72	0.322
CC–CW	0.268	0.158	69	1.70	0.333
CC–WW	0.791	0.144	69	5.51	**<0.0001**
WC–CW	0.020	0.157	69	0.13	0.999
WC–WW	0.543	0.143	69	3.79	**0.0018**
CW–WW	0.523	0.156	69	3.36	**0.0068**